Biophysical Journal
Article

Biophysical Society

Mechanics and Actomyosin-Dependent Survival/Chemoresistance of Suspended Tumor Cells in Shear Flow

Ying Xin,[1,2] Xi Chen,[1,2] Xin Tang,[2] Keming Li,[1,2] Mo Yang,[2] William Chi-Shing Tai,[3] Yiyao Liu,[4] and Youhua Tan[1,2,*]

[1]The Hong Kong Polytechnic University Shenzhen Research Institute, Shenzhen, China; [2]Department of Biomedical Engineering, The Hong Kong Polytechnic University, Hong Kong, China; [3]Department of Applied Biology and Chemical Technology, The Hong Kong Polytechnic University, Hong Kong, China; and [4]University of Electronic Science and Technology of China, Chengdu, China

ABSTRACT Tumor cells disseminate to distant organs mainly through blood circulation in which they experience considerable levels of fluid shear stress. However, the effects of hemodynamic shear stress on biophysical properties and functions of circulating tumor cells (CTCs) in suspension are not fully understood. In this study, we found that the majority of suspended breast tumor cells could be eliminated by fluid shear stress, whereas cancer stem cells held survival advantages over conventional cancer cells. Compared to untreated cells, tumor cells surviving shear stress exhibited unique biophysical properties: 1) cell adhesion was significantly retarded, 2) these cells exhibited elongated morphology and enhanced spreading and expressed genes related to epithelial-mesenchymal transition or hybrid phenotype, and 3) surviving tumor cells showed reduced F-actin assembly and stiffness. Importantly, inhibiting actomyosin activity promoted the survival of suspended tumor cells in fluid shear stress, whereas activating actomyosin suppressed cell survival, which might be explained by the up- and downregulation of the antiapoptosis genes. Soft surviving tumor cells held survival advantages in shear flow and higher resistance to chemotherapy. Inhibiting actomyosin activity in untreated cells enhanced chemoresistance, whereas activating actomyosin in surviving tumor cells suppressed this ability. These findings might be associated with the corresponding changes in the genes related to multidrug resistance. In summary, these data demonstrate that hemodynamic shear stress significantly influences biophysical properties and functions of suspended tumor cells. Our study unveils the regulatory roles of actomyosin in the survival and drug resistance of suspended tumor cells in hemodynamic shear flow, which suggest the importance of fluid shear stress and actomyosin activity in tumor metastasis. These findings may reveal a new, to our knowledge, mechanism by which CTCs are able to survive hemodynamic shear stress and chemotherapy and may offer a new potential strategy to target CTCs in shear flow and combat chemoresistance through actomyosin.

INTRODUCTION

Metastasis is a complex process, mainly including the detachment of tumor cells from primary lesions, invasion into tumor stroma, intravasation into the vascular system, survival in circulation, extravasation into distant organs, and formation of metastatic tumors (1). Tumor cells metastasize to distant organs mainly through hematogenous dissemination in which the frequency of circulating tumor cells (CTCs) is correlated with poor prognosis and overall survival in cancer patients (2,3). CTCs are heterogeneous with diverse subpopulations of distinct genotypes and phenotypes (4,5). Less than 0.01% of them may eventually generate metastatic tumors in secondary sites, indicating the inefficiency of metastasis (1). Nevertheless, metastasis accounts for more than 90% of cancer-related deaths (1), suggesting that a subpopulation of CTCs are able to survive the metastatic process and form metastases. To target metastasis, it is thus essential to understand the roles of various factors during dissemination in the survival and functions of CTCs.

Apart from many biochemical factors that affect CTC functions and metastasis (6), cells are able to sense and respond to forces through mechanotransduction (7) that regulate mRNA transcription and cellular functions (8,9).

Submitted January 7, 2019, and accepted for publication April 3, 2019.

*Correspondence: youhua.tan@polyu.edu.hk

Editor: Jochen Guck.

https://doi.org/10.1016/j.bpj.2019.04.011

© 2019 Biophysical Society.

Emerging evidence has demonstrated that mechanical factors play important roles in tumor metastasis (10,11), including fluid shear stress that tumor cells experience in blood circulation, which is hypothesized to affect the survival and functions of CTCs. Fluid shear stress significantly influences the functions of tumor cells that are adhered to solid substrates. High levels of shear stress promote the production of reactive oxygen species in lung cancer cells and induce cell damage (12). Fluid shearing sensitizes cancer cells to radiation-induced apoptosis by regulating integrin and focal adhesion kinase activity (13). Shear forces modulate global gene expression and affect the proliferation of colon cancer cells (14). Interstitial shear flow arrests tumor cell cycle and proliferation through integrin and Smad (15). Shear stress gradients stimulate the expression of insulin-like growth factor-1 and proliferation of Ewing sarcoma cells (16). Shear stress in lymphatic vasculature regulates ROCK-YAP1 signaling and enhances cancer cell migration (17). Shear flow increases the secretion of matrix metalloproteinases and cancer cell invasion (18). Fluid flow facilitates epithelial-mesenchymal transition (EMT) and cell mobility (19) and confers tumor cells CSC properties (20). However, the effects of fluid shear stress on tumor cells in suspension remain less understood. The viability and proliferation of colon CTCs are related to the magnitude of shear stress and circulating time (21). Shear stress sensitizes suspended colon and prostate tumor cells to apoptosis (22). High fluid shear stress induces considerable levels of apoptosis in tumor cells (23) and facilitates migration and extravasation (24). Malignant tumor cells exhibit resistance to hemodynamic shear stress, which is regulated by transforming oncogenes (25) and nuclear lamin A/C (26). Nevertheless, the influence of hemodynamic shear stress on biophysical properties and chemoresistance of CTCs remains elusive. The roles of cell mechanics in the survival and drug resistance of CTCs in fluid shear flow are unclear.

In this study, we developed a circulatory system to generate physiologic levels of hemodynamic shear stress, which mimicked certain important aspects of the CTC microenvironment in blood circulation. The survival of tumor cells in suspension, as a model for real CTCs, under different shear stress and circulation duration was examined. The properties of tumor cells surviving hemodynamic shear stress were characterized, including adhesion, morphology, spreading, cytoskeleton, cellular stiffness, and chemoresistance. Importantly, the roles of actomyosin activity in the survival of suspended tumor cells in fluid shear stress and in drug resistance of surviving tumor cells were elucidated.

MATERIALS AND METHODS

Cell culture

Human breast cancer cell lines MDA-MB-468, MCF-7, MDA-MB-231, and MDA-MB-453 were purchased from ATCC (Manassas, VA). Cells were maintained with Dulbecco's Modified Eagle Medium (DMEM; HyClone Laboratories, Logan, UT) supplemented with 10% fetal bovine serum (HyClone Laboratories) and 1% penicillin/streptomycin (HyClone Laboratories) in petri dishes at 37°C and 5% CO_2. Cells were passaged every 2–3 days using 0.25% trypsin (HyClone Laboratories).

Shear stress treatment

The circulatory system consisted of a peristaltic pump (P-230; Harvard Apparatus, Holliston, MA), a silicone microtubing (0.51 mm in diameter and 1.5 m in length), and a syringe as cell solution reservoir. The system could generate pulsatile flow, which mimicked hemodynamic shear stress in blood circulation. According to Poiseuille's law, wall shear stress τ (dyne/cm^2) in the tubing was calculated by $\tau = 4\mu Q/(\pi R^3)$, where Q is the flow rate (from 0.001 to 230 mL/min), μ is the dynamic viscosity of the fluid (0.01 dyne • s/cm^2 for cell culture medium), and R is the radius of the tube (0.255 mm). The whole system was sterilized by 75% ethanol before experiments and then rinsed with 4 mL phosphate buffered saline (HyClone Laboratories). To reduce the adhesion of suspended tumor cells to the tube and syringe, the system was washed with 4 mL 1% bovine serum albumin (VWR Life Science, Radnor, PA). During experiments, 2 mL cell suspension solution (2×10^5 cells/mL) was added into the circulatory system and subjected to various magnitudes of shear stress for different durations (0–20 dyne/cm^2; 0–24 h) in the cell culture incubator at 37°C and 5% CO_2.

Pharmacologic treatment and plasmid transfection

For pharmacologic treatment, cells were treated with 2 μM Y-27632 (Selleck Chemicals, Houston, TX), 4 μM blebbistatin (Sigma, St. Louis, MO), 0.3 μM cytochalasin D (Tocris Bioscience, Bristol, United Kingdom), and 10 or 50 μM 5-FU (Tocris Bioscience) for different durations. Lipofectamine 3000 reagent (Thermo Fisher Scientific, Waltham, MA) was used for plasmid transfection, including pSLIK-Venus, pSLIK CA-ROCK, and pSLIK CA-MLCK (gifts from professor Sanjay Kumar). In brief, cells were seeded in a 24-well plate until 70–90% of confluence was reached. Lipofectamine 3000 reagent and plasmids were diluted using Opti-MEM, respectively. Diluted plasmids were then mixed with P3000 reagent. The same amount of Lipofectamine 3000 and plasmids was mixed and incubated at room temperature for 15 min. The plasmid-lipid mixture was used to transfect cells for 2 days, when 50 ng/mL doxycycline (TargetMol, Wellesley, MA) was added for another 2 days.

MTS assay

Cell viability was measured by MTS assay (Promega, Madison, WI) following the manufacturer's instructions. Briefly, 100 μL of cell suspension was collected from the circulatory system and then added into 1 well in a 96-well plate. After 12 h of incubation, 20 μL of sterilized CellTiter 96 Aqueous One Solution (5 mg/mL; Promega) was added to each well, and the plate was incubated at 37°C for 4 h. The absorbance of the cell solution was measured at 490 nm using a Benchmark Plus microplate reader (Bio-Rad, Hercules, CA).

Quantification of cell adhesion

For cell adhesion, the culture medium was changed to DMEM without fetal bovine serum at 8 h before the assay. The 96-well plate was pretreated with 40 μg/mL collagen I solution (Corning, Corning, NY) at 4°C for 12 h. Cells obtained from various conditions were resuspended in 0.1% bovine serum albumin and DMEM and added into the treated

96-well plate. After plating for different durations, supernatant containing nonadherent cells was removed and fresh culture medium was added. For each condition, the same number of cells were cultured for 24 h without removing supernatant, which were used as a reference. Cells were incubated for another 12 h, after which the quantification of cell adhesion was measured by MTS assay. The percentage of adhered cells was calculated by the ratio of MTS reading over the reference under the same condition.

Quantitative RT-PCR analysis

Total mRNAs were extracted by Aurum Total RNA Mini Kit (Bio-Rad), and complementary DNA was synthesized using RevertAid First Strand cDNA Synthesis Kit (Thermo Fisher Scientific) according to the manufacturer's instructions, respectively. Quantitative RT-PCR was performed using Forget-Me-Not EvaGreen qPCR Master Mix with Rox (Biotium, Fremont, CA) and CFX96 Real-Time PCR Detection System (Bio-Rad). The sequences of all the primers were obtained from the National Center for Biotechnology Information database and listed in Table S1. For data analysis, the expressions of all genes were normalized using the $\Delta\Delta$cycle threshold method against human glyceraldehyde 3-phosphate dehydrogenase.

Western blotting

Cells were lysed by radioimmunoprecipitation assay lysis and extraction buffer (Solarbio Life Sciences, Beijing, China) together with Halt Phosphatase Inhibitor Cocktail (Thermo Fisher). About 50 μg of total protein was transferred from 10% sodium dodecyl sulfate polyacrylamide gel electrophoresis gel to a polyvinylidene difluoride Western blot membrane using Trans-Blot Turbo (Bio-Rad). The membrane was incubated with TBST/5% nonfat milk (Solarbio Life Sciences) and stained with different primary antibodies (E-cadherin, Twist, Tubulin (Abcam, Cambridge, MA)) and secondary antibodies (Goat Anti-Mouse Immunoglobulin G (H + L)-HRP Conjugate and Goat Anti-Rabbit Immunoglobulin G (H + L)-HRP Conjugate (Bio-Rad)). Images were taken using Clarity and Clarity Max Western Enhanced Chemiluminescence Blotting Substrates and ChemiDoc MP Imaging System (Bio-Rad).

F/G-actin ratio measurement

F-actin/G-actin ratio was measured by G-actin/F-actin In Vivo Assay Kit (Cytoskeleton, Denver, CO) under the manufacturer's instructions. Briefly, cells after different treatment were lysed in Lysis and F-actin Stabilization Buffer (Cytoskeleton) combined with ATP solution and protease inhibitor cocktail and centrifuged at 2000 rotations per minute for 5 min at room temperature. Then, the supernatant was transferred to an ultrafast centrifuge tube and centrifuged at 100,000 $\times$ g for 1 h to pellet F-actin from soluble G-actin. F-actin depolymerization buffer was added to the F-actin pellet on ice for 1 h. The expression of F-actin and G-actin protein was analyzed by Western blotting as described above.

Annexin V assay

Apoptosis assay was performed using Annexin V-fluorescein isothiocyanate (FITC) Apoptosis Staining/Detection Kit (Abcam) and BD Accuri C6 Flow Cytometer (BD Biosciences, San Jose, CA). 100,000 cells were collected and resuspended in 500 μL of 1$\times$ Binding Buffer (Abcam). Then, 5 μL of Annexin V-FITC and 5 μL of propidium iodide were added into cell solution and incubated in the dark for 5 min. 10,000 cells were counted for analyzing Annexin V-FITC binding by FITC signal detector and propidium iodide staining by the phycoerythrin signal detector. The results were analyzed by BD Accuri C6 software.

Quantification of cell morphology and spreading

Tumor cells were exposed to 0 or 20 dyne/cm^2 shear stress for 12 h and then plated into petri dishes. At least 100 cells/condition were imaged by the inverted microscope (Nikon, Tokyo, Japan) after different durations of incubation. Cell aspect ratio and spreading area were quantified by the ImageJ software (National Institutes of Health, Bethesda, MD).

Statistical analysis

Two-tailed Student's t-test or analysis of variance (ANOVA) was used for the statistics among two or more conditions. The post hoc Tukey or Bonferroni test was adopted in the ANOVA analysis for the comparisons with equal or unequal sample sizes, respectively.

Note that more methods can be found in Supporting Materials and Methods.

RESULTS

The majority of suspended tumor cells can be eliminated by hemodynamic shear stress dependent on shear stress and circulation duration

To explore the influence of fluid shear stress on CTCs, we developed a circulatory system (Fig. S1), which included a peristaltic pump, a silicone microtubing, and a syringe as cell solution reservoir. The system could generate pulsatile flow at 37°C and 5% CO_2, which mimicked shear stress in blood circulation. The wall shear stress τ in tubing was calculated according to $\tau = 4\mu Q/(\pi R^3)$ (21), where μ is the fluid viscosity (0.01 dyne $\cdot$ s/cm^2 for the medium), Q is the flow rate, and R is the tubing radius (0.255 mm). To be physiologically relevant, fluid shear stress within 20 dyne/cm^2 and circulation duration within 12 h were chosen in this study (2,21). Note that it is challenging to experimentally measure local shear stress experienced by single tumor cells.

Our data show that the viability of breast cancer cells MDA-MB-468 in suspension gradually decreased to $\sim$21% when hemodynamic shear stress and circulating time increased from 0 to 20 dyne/cm^2 and from 0 to 12 h, respectively (Fig. 1 *a*). Similar findings were also observed in several other types of breast cancer cells, including MCF-7, MDA-MB-453, and MDA-MB-231 (Fig. 1, *b* and *c*; Fig. S2 *a*), suggesting that fluid shear stress eliminates the majority of CTCs dependent on the magnitudes of shear stress and circulation duration. Cancer stem cells (CSCs) have been proposed to initiate metastatic tumors (27) and thus must have the survival advantages during the whole metastatic process, including blood circulation. To this end, tumorigenic CSCs were selected from MDA-MB-468 and MCF-7 cells by three-dimensional soft fibrin gels as we developed previously (28,29). These fibrin-selected CSCs exhibited much higher self-renewal (Fig. S3) (28,29) and remarkably higher viability in fluid shear flow than conventional tumor cells (Fig. 1 *d*; Fig. S2 *b*), suggesting that CSCs hold survival advantages in blood shear flow.

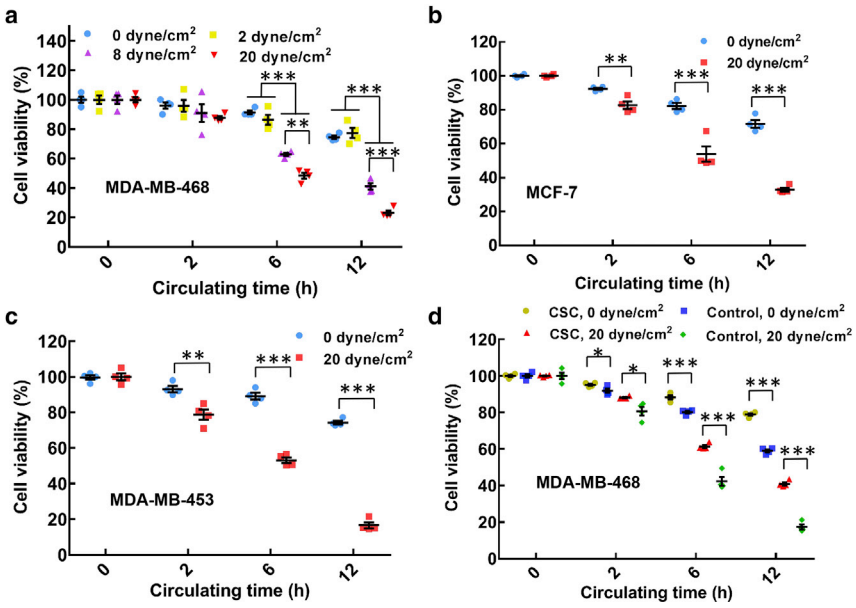

FIGURE 1 The majority of suspended tumor cells can be eliminated by hemodynamic shear flow dependent on the magnitudes of shear stress and circulation duration. (*a–c*) The viability of breast cancer cells in suspension decreases along with fluid shear stress and circulation duration. Single cell suspensions of MDA-MB-468 (*a*), MCF-7 (*b*), and MDA-MB-453 (*c*) were obtained by trypsinization from petri dish and circulated under various magnitudes of shear stress and circulation duration. The viability of treated cells was measured by MTS assay and normalized by the data at 0 h under the same treatment; $n = 4$ independent experiments. (*d*) Fibrin-selected cancer stem cells (CSCs) exhibit considerable survival advantage in hemodynamic shear flow over nonselected cells. Breast cancer cells MDA-MB-468 were cultured in soft (90 Pa) fibrin gels for 7 days. Suspended fibrin-selected cells (CSCs) and tumor cells cultured in petri dish (control) were treated under 0 and 20 dyne/cm^2 shear stress, respectively; $n = 4$ independent experiments. The statistics were conducted using ANOVA with the post hoc Tukey test in (*a*) and two-tailed Student *t*-test in (*b*)–(*d*). $*p < 0.05$; $**p < 0.01$; $***p < 0.001$. The data in the figures of this paper represent mean ± SEM (standard error of the mean). To see this figure in color, go online.

Tumor cells surviving hemodynamic shear stress exhibit unique biophysical properties

Although the majority of tumor cells in circulation can be eliminated by hemodynamic shear stress, a minor subpopulation of cells persist in the heterogeneous CTCs that may eventually generate metastatic tumors. It is thus crucial to characterize the functions of these surviving tumor cells. To this end, their biophysical properties were examined, including cell adhesion, morphology, spreading, cytoskeleton, and cellular stiffness. The data show that compared to untreated cells ("control"), the adhesion to solid substrates was considerably suppressed at 2 h after plating for tumor cells treated by 0 dyne/cm^2 shear stress and at 2, 4, and 8 h for cells treated by 20 dyne/cm^2 shear stress (Fig. 2, *a* and *b*). Significant differences were found in cell adhesion at 2 and 4 h between cells treated by 0 and 20 dyne/cm^2 shear stress (Fig. 2 *b*). The adhesion of these tumor cells was increased to the similar level of untreated cells at 4 and 12 h after plating, respectively. These findings suggest that the adhesion of tumor cells surviving fluid shear flow may be significantly inhibited at early phase but restored to the normal level at late phase.

After culture on solid substrates, cell morphology and spreading were examined. We found that although cell adhesion was suppressed at an early phase for tumor cells surviving shear stress treatment (0 and 20 dyne/cm^2), the morphology of the adhered cells was notably more elongated than untreated MDA-MB-468 (except 0 dyne/cm^2 at 8 h; Fig. 3, *a* and *b*) and MCF-7 cells (except 0 dyne/cm^2 at 12 h; Figs. S4, *a* and *b*). The spreading area of these surviving tumor cells was significantly increased, especially after 4 h postplating for MDA-MB-468 and MCF-7 cells (Fig. 3 *c*; Fig. S4 *c*). Compared to the cells after 0 dyne/cm^2 shear stress treatment, tumor cells surviving 20 dyne/cm^2 shear stress exhibited a higher aspect ratio at 2 and 20 h for MDA-MB-468 and at 1, 4, 12, and 20 h for MCF-7 cells and spread more for MDA-MB-468 (except at 20 h) and at 4, 12, and 20 h for MCF-7 cells. The findings of elongated cell morphology and enhanced spreading suggest that tumor cells surviving hemodynamic shear stress may undergo EMT. To explore this possibility, we examined the expression of EMT genes. Compared to untreated cells, surviving tumor cells expressed lower epithelial cell marker E-cadherin and higher mesenchymal cell marker Twist at the protein level (Fig. 3 *d*, *top panel*). Note that tumor cells expressed higher levels of both E-cadherin and Twist after the treatment under 20 dyne/cm^2 shear stress than 0 dyne/cm^2 shear stress, representative of a hybrid epithelial/mesenchymal phenotype. Further, E-cadherin was significantly downregulated, and the mesenchymal cell markers fibronectin, Twist, and vimentin were notably upregulated in surviving tumor cells at the mRNA level (Fig. 3 *d*, *bottom panel*). All these data suggest that fluid shear stress may promote EMT or hybrid epithelial/mesenchymal phenotype in surviving tumor cells.

Cell morphology and spreading are closely related to cytoskeletal structures. Compared to untreated cells, F-actin assembly and the F-actin/G-actin ratio were notably decreased in tumor cells after shear stress treatment, as measured by both immunofluorescence and Western blotting

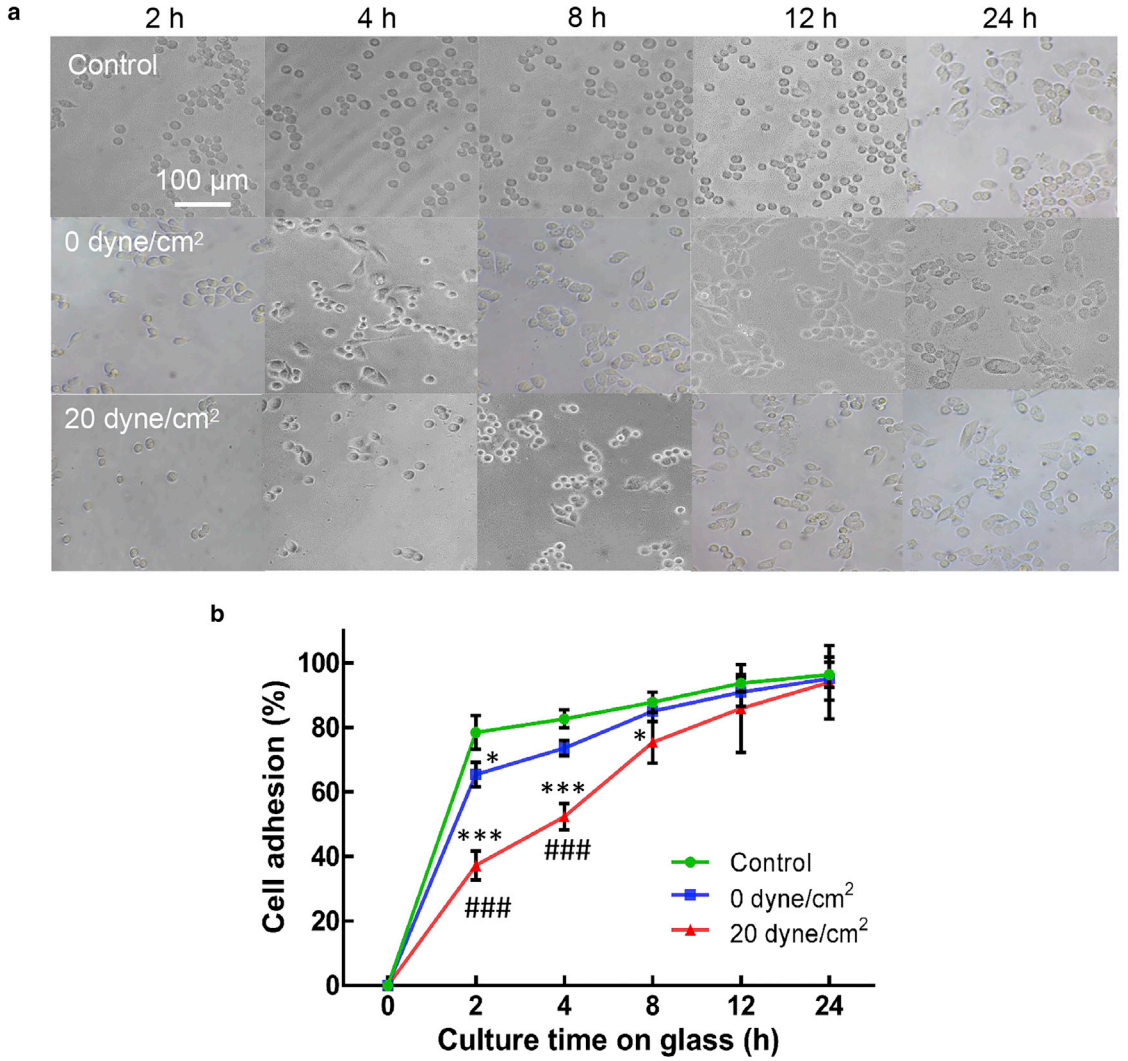

FIGURE 2 Hemodynamic shear stress retards the adhesion of suspended tumor cells. (*a*) Representative images of tumor cell adhesion after shear stress treatment are shown. Suspended MDA-MB-468 cells were circulated under 0 and 20 dyne/cm^2 shear stress for 12 h, respectively. Tumor cells cultured in petri dish were used as a control. The treated and control cells were then cultured on collagen-coated glass for 2, 4, 8, 12, and 24 h, respectively. Nonadhered cells were removed by gentle washing before imaging. Scale bars, 100 μm. (*b*) The quantification of tumor cell adhesion is shown. The percentage of the adhered cells was calculated by the ratio of the MTS reading at the indicated time point over the reading of cells at 24 h after plating under the same condition ($n = 3$ wells for each condition). The statistics were conducted using ANOVA with the post hoc Tukey test. $^*p < 0.05$ and $^{***}p < 0.001$ shows significant differences between "control" and "0 " or "20 dyne/cm^2," and $^{\#\#\#}p < 0.001$ shows significant differences between "0 " and "20 dyne/cm^2." $n = 3$ independent experiments. To see this figure in color, go online.

(Fig. 4, *a* and *b*; Fig. S5). Tumor cells surviving 20 dyne/cm^2 shear stress exhibited significantly lower F-actin and F-actin/G-actin ratio (~0.38 vs ~0.64) than the cells after 0 dyne/cm^2 shear stress treatment. These findings suggest that fluid shear stress may remodel the cytoskeleton of suspended tumor cells. Because cytoskeleton largely determines cell mechanics (30), we further explored whether surviving tumor cells with remodeled cytoskeleton exhibited unique mechanical properties. The results of atomic force microscopy measurement show that the force-indentation curves of tumor cells after shear stress treatment had significantly lower values of slope (Fig. 4 *c*). By fitting the data with the modified Hertz model (31), Young's modulus was characterized. The results show that surviving tumor cells (20 dyne/cm^2) were notably softer than tumor cells after suspension treatment (0 dyne/cm^2) and untreated cells (~1600 Pa vs ~2000 and ~2300 Pa; Fig. 4 *d*). These data suggest that suspended tumor cells surviving hemodynamic shear stress are much softer with reduced F-actin assembly.

Actomyosin activity regulates the survival of suspended tumor cells in hemodynamic shear stress

We have shown that hemodynamic shear stress considerably influences the survival of suspended tumor cells and that

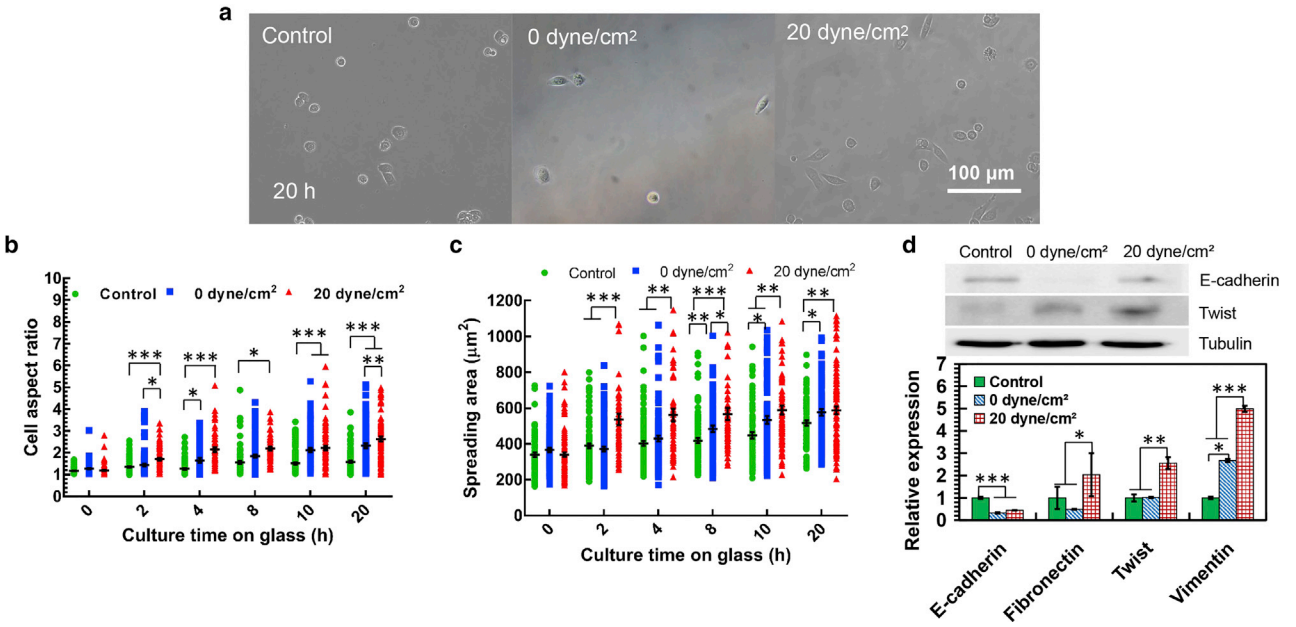

FIGURE 3 Hemodynamic shear stress influences the epithelial/mesenchymal phenotype of suspended tumor cells. (*a*) Representative images of tumor cell morphology after shear stress treatment are shown. Suspended MDA-MB-468 cells treated under different shear stresses were cultured on collagen-coated glass. Cell images were taken at the indicated time points after removing nonadhered cells. Scale bar, 100 μm. (*b* and *c*) Fluid shear stress promotes elongated morphology and spreading of circulating tumor cells (CTCs). The aspect ratio (*b*) and spreading area (*c*) of the treated tumor cells in (*a*) were quantified ($n > 92$); $n = 3$ independent experiments. (*d*) Fluid shear stress influences the expressions of mesenchymal/epithelial genes in CTCs. The expressions of epithelial marker (E-cadherin) and mesenchymal markers (Twist, fibronectin, and vimentin) in surviving tumor cells were measured by quantitative RT-PCR. E-cadherin and Twist were analyzed by Western blotting; $n = 2$ and 3 independent experiments for the top and bottom panels, respectively. The statistics were conducted using ANOVA with the post hoc Bonferroni test in (*b*) and (*c*) and Tukey test in (*d*). $^{*}p < 0.05$; $^{**}p < 0.01$; $^{***}p < 0.001$. To see this figure in color, go online.

surviving tumor cells exhibit unique biophysical properties, including the reduced F-actin and cell stiffness. However, the roles of cell mechanics in the survival of CTCs in shear flow remain unclear. To address this problem, the cytoskeleton and mechanics of tumor cells were modulated by targeting actomyosin activity. The data show that pharmacologically inhibiting actomyosin by Rho-associated protein kinase (ROCK) inhibitor Y27632, myosin II inhibitor blebbistatin, or F-actin inhibitor cytochalasin D reduced F-actin assembly (Fig. S6) but notably enhanced the viability of suspended breast tumor cells (MDA-MB-468 and MCF-7) in fluid shear flow (Fig. 5 *a*; Fig. S7 *a*; except Y27632 in Fig. S7 *a*). This effect was further confirmed by the Annexin V apoptosis assay (Fig. S8). On the other hand, activating actomyosin by expressing constitutive active (CA) mutants of myosin light-chain kinase (MLCK) or ROCK significantly increased F-actin assembly and the F-actin/G-actin ratio (Fig. S9) but suppressed tumor cell survival in hemodynamic shear stress (Fig. 5 *b*; Fig. S7 *b*; except CA-MLCK at 12 h in Fig. 5 *b* and in Fig. S7 *b*). These findings suggest that low/high actomyosin activity promotes/inhibits the survival of suspended tumor cells in blood shear flow.

Tumor cells surviving shear stress exhibited low stiffness (Fig. 4). We wondered whether these soft tumor cells possessed survival advantages in blood shear flow. The data show that surviving tumor cells held remarkably higher viability in shear flow compared to control tumor cells (Fig. 5 *c*). CSCs are known to have lower stiffness than bulk tumor cells (28,29). We have demonstrated that CSCs survive much better in fluid shear flow (Fig. 1 *d*; Fig. S2 *b*). Activating actomyosin significantly reduced the survival of CSCs in shear stress (Fig. S7 *c*). To explore the underlying survival mechanisms, the antiapoptosis genes were examined, including B-cell lymphoma 2 (Bcl2) and superoxide dismutase 2 (SOD2; mitochondrial). We found that tumor cells after treatment by 20 dyne/cm^2 shear stress showed considerable increase in the expressions of these genes compared to control cells and tumor cells treated in suspension (Fig. 5 *d*; Fig. S10). Inhibiting actomyosin significantly increased the expressions of Bcl2 and SOD2 (Fig. 5 *d*; Fig. S11), whereas activating actomyosin activity suppressed their expressions (Fig. 5 *e*; Fig. S12). These data suggest that actomyosin regulates the survival of suspended tumor cells in fluid shear flow probably via the effects on antiapoptosis genes.

Suspended tumor cells surviving hemodynamic shear stress exhibit actomyosin-dependent chemoresistance

Research and clinical findings have demonstrated that metastatic tumors exhibit high levels of resistance to

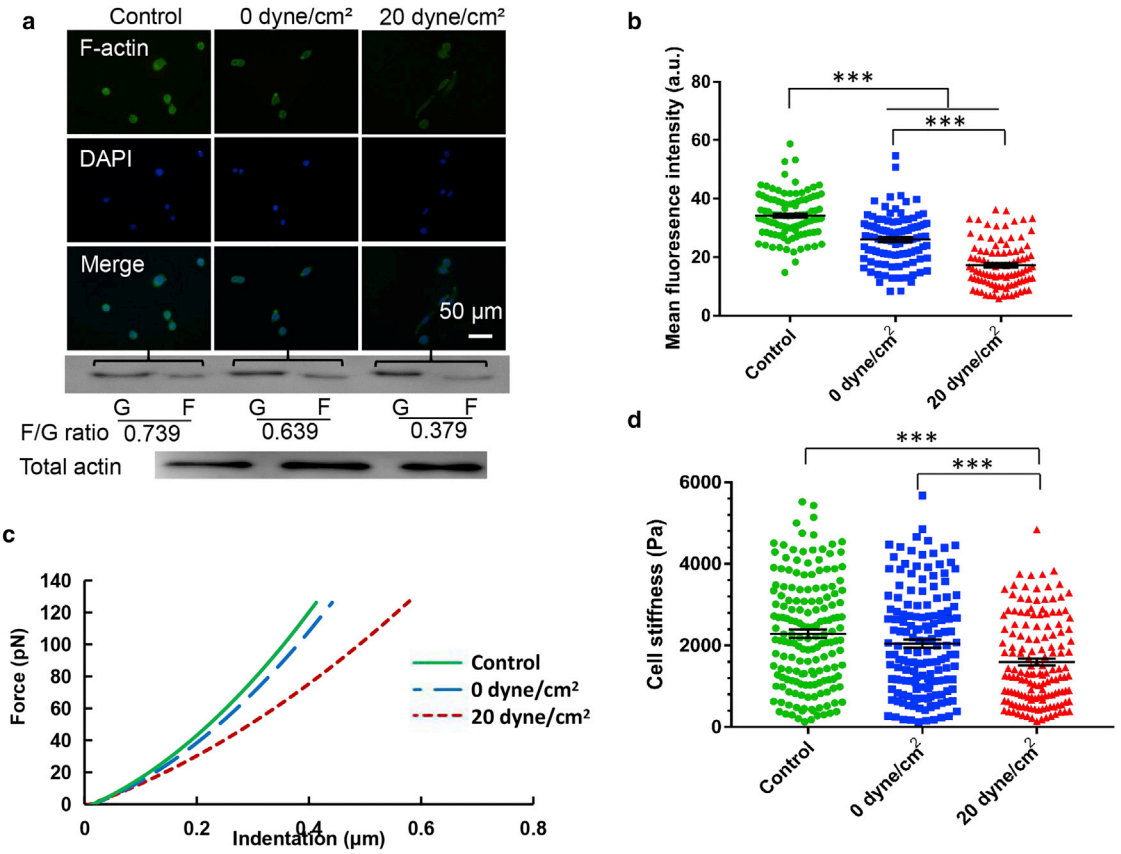

FIGURE 4 Suspended tumor cells surviving fluid shear stress exhibit reduced F-actin assembly and cell stiffness. (*a*) Immunofluorescence imaging and immunoblotting of F-actin in breast cancer cells after shear stress treatment are shown. MDA-MB-468 cells were treated under 0 and 20 dyne/cm^2 shear stress for 12 h and then plated on glass for 10 h, after which F-actin was stained and the immunoblotting of G-actin (G) and F-actin (F) was conducted. The level of total actin was used as a control. The value represents the F-actin/G-actin ratio; $n = 2$ independent experiments. The nucleus was counterstained with 4′,6-diamidino-2-phenylindole (DAPI). Scale bars, 50 μm. (*b*) Surviving tumor cells show much lower F-actin assembly. F-actin in the top panel of (*a*) was quantified ($n > 100$); $n = 3$ independent experiments. (*c*) Typical force-indentation curves of breast cancer cells after shear stress treatment measured by atomic force microscopy are shown. (*d*) Breast cancer cells surviving hemodynamic shear stress exhibit much lower stiffness. MDA-MB-468 cells after shear stress treatment were plated on glass for 10 h, after which cell stiffness was measured. At least 150 cells were measured for each condition; $n = 3$ independent experiments. The statistics were conducted using ANOVA with the post hoc Bonferroni test in (*b*) and (*d*). ***$p < 0.001$. a.u., arbitrary unit. To see this figure in color, go online.

conventional chemotherapy (32–34), which is one major cause of recurrence and cancer-induced death. Tumor cells with the ability to generate metastases must survive the entire metastatic process, including blood circulation, and may be responsible for drug resistance of metastatic tumors. We thus hypothesized that tumor cells surviving hemodynamic shear stress might possess the ability to resist chemotherapy. To test this idea, breast cancer cells surviving 0 and 20 dyne/cm^2 shear stress were treated with different doses of conventional chemotherapy drug fluorouracil (5-FU). The data show that surviving tumor cells exhibited remarkably higher viability than untreated cells after chemotherapy (Fig. 6 *a*; Fig. S13 *a*), suggesting that tumor cells surviving blood shear flow or suspension hold considerable chemoresistance advantage. Note that there was no significant difference in drug resistance between 0 and 20 dyne/cm^2 shear stress treatment. We have shown that these surviving tumor cells exhibit low F-actin and stiffness. However, the roles of cell mechanics in chemoresistance of CTCs remain unclear. Our results show that activating CA-ROCK or CA-MLCK in soft surviving tumor cells significantly decreased cell viability after chemotherapy (Fig. 6 *b*; Fig. S13 *b*), suggesting that high actomyosin activity suppresses chemoresistance. Further, pharmacologic inhibition of actomyosin in untreated breast cancer cells remarkably enhanced resistance to chemotherapy (Fig. 6 *c*; Fig. S13 *c*). These findings demonstrate that actomyosin activity regulates chemoresistance of tumor cells surviving fluid shear flow. To explore the underlying mechanisms, the genes related to multidrug resistance (MDR) were examined. The data show that tumor cells after 5-FU treatment and the cells surviving shear stress upregulated the expressions of MDR genes in both MDA-MB-468 (MRP3, GSTP1, ABCG2, and MRP1) and MCF-7 cells (ABCG2 and MRP3) (Fig. 6 *d*; Figs. S13 *d* and S14 *a*). Pharmacologically inhibiting actomyosin upregulated the expressions of MDR genes (Fig. 6 *d*; Figs. S13

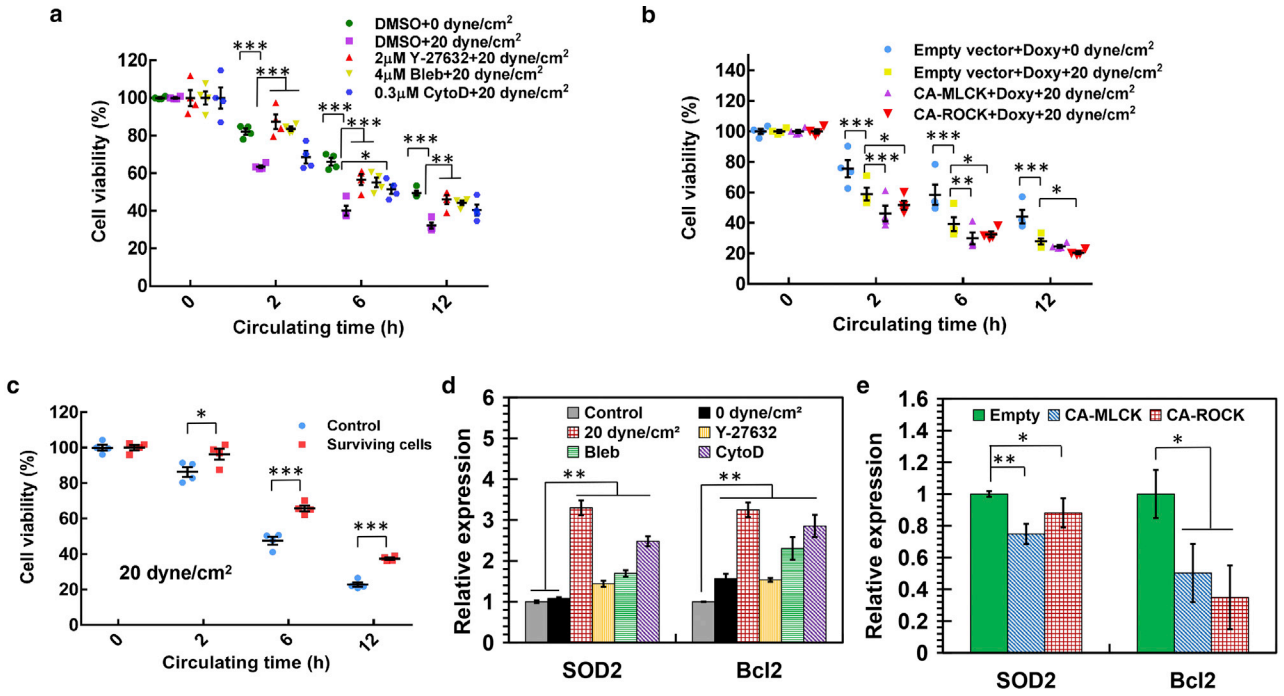

FIGURE 5 Actomyosin activity regulates the survival of suspended tumor cells in hemodynamic shear stress. (*a*) Pharmacologically inhibiting actomyosin enhances the viability of suspended breast tumor cells in fluid shear flow. MDA-MB-468 cells were treated with 2 μM Y-27632, 4 μM blebbistatin (Bleb), or 0.3 μM cytochalasin D (CytoD) for 48 h and then circulated under 20 dyne/cm^2 shear stress with the inhibitor for the indicated durations. Cell viability was measured by MTS assay (three wells per condition); $n = 4$ independent experiments. (*b*) Activating actomyosin suppresses the survival of suspended breast tumor cells in fluid shear flow. Tumor cells were transfected with constitutive active (CA) MLCK or ROCK in the presence of doxycycline (Doxy) and then circulated under 20 dyne/cm^2 shear stress with doxycycline. Cell viability was measured by MTS assay; $n = 4$ independent experiments. (*c*) Tumor cells surviving shear flow hold survival advantages in hemodynamic shear stress. MDA-MB-468 cells were circulated under 20 dyne/cm^2 shear stress for 12 h. The surviving cells were cultured in petri dish for 10 h, and the retrieved suspended cells were then retreated under 20 dyne/cm^2 shear stress. Tumor cells that were cultured in petri dish were used as a control; $n = 4$ independent experiments. (*d*) Shear stress or inhibition of actomyosin upregulates the antiapoptosis genes. MDA-MB-468 cells were treated with various inhibitors for 48 h as in (*a*) or circulated in 0 and 20 dyne/cm^2 shear stress for 12 h, respectively. The treated cells were collected for the analysis of antiapoptosis genes Bcl2 and SOD2; $n = 3$ independent experiments. (*e*) Actomyosin activation in tumor cells suppresses the expressions of antiapoptosis genes. MDA-MB-468 cells were transfected with CA-MLCK or CA-ROCK with doxycycline for 48 h, after which the gene expressions were examined; $n = 3$ independent experiments. The statistics were conducted using ANOVA with the post hoc Tukey test in (*a*), (*b*), (*d*), and (*e*) and two-tailed Student *t*-test in (*c*). *$p < 0.05$; **$p < 0.01$; ***$p < 0.001$. To see this figure in color, go online.

d and S14 *b*), whereas activating ROCK but not MLCK significantly suppressed these genes (Fig. 6 *e*; Fig. S15). These findings suggest that suspended tumor cells surviving hemodynamic shear stress hold chemoresistance ability in an actomyosin-dependent manner.

DISCUSSION

Tumor cells disseminate to distant organs mainly through blood circulation during metastasis (1) in which they experience considerable levels of fluid shear stress. It is documented that mechanical factors play important roles in tumor progression and metastasis (10,11). Fluid shear stress significantly affects the survival, proliferation, and other functions of adhered and suspended cells (21–25,35,36). Consistently, our study shows that the majority of tumor cells in suspension can be eliminated by fluid shear flow, suggesting that hemodynamic shear stress could be one major cause for the poor survival of CTCs in vasculature and metastasis inefficiency. Nevertheless, a small subpopulation of tumor cells are able to survive in fluid shear flow, which may enrich tumor cells with the ability to generate metastatic tumors. However, the biophysical properties of these cells remain poorly characterized. This study shows that tumor cells surviving suspension or shear flow appear to be mesenchymal-like or hybrid epithelial/mesenchymal, which is different from the reported finding (35), possibly because of distinct fluid shear conditions. Note that fluid shear flow induces a hybrid epithelial/mesenchymal phenotype in suspended tumor cells compared to suspension. It is still unclear how shear stress influences the EMT phenotype of suspended tumor cells. It is possible that fluid shear flow selects a subpopulation of preexisting cells with mesenchymal or hybrid phenotype or induces the phenotypic changes, which needs to be further tested in the future. Compared to the suspension condition, cell cytoskeleton is further remodeled after shear stress treatment, especially the reduced F-actin, which may lead to the decrease in cellular stiffness

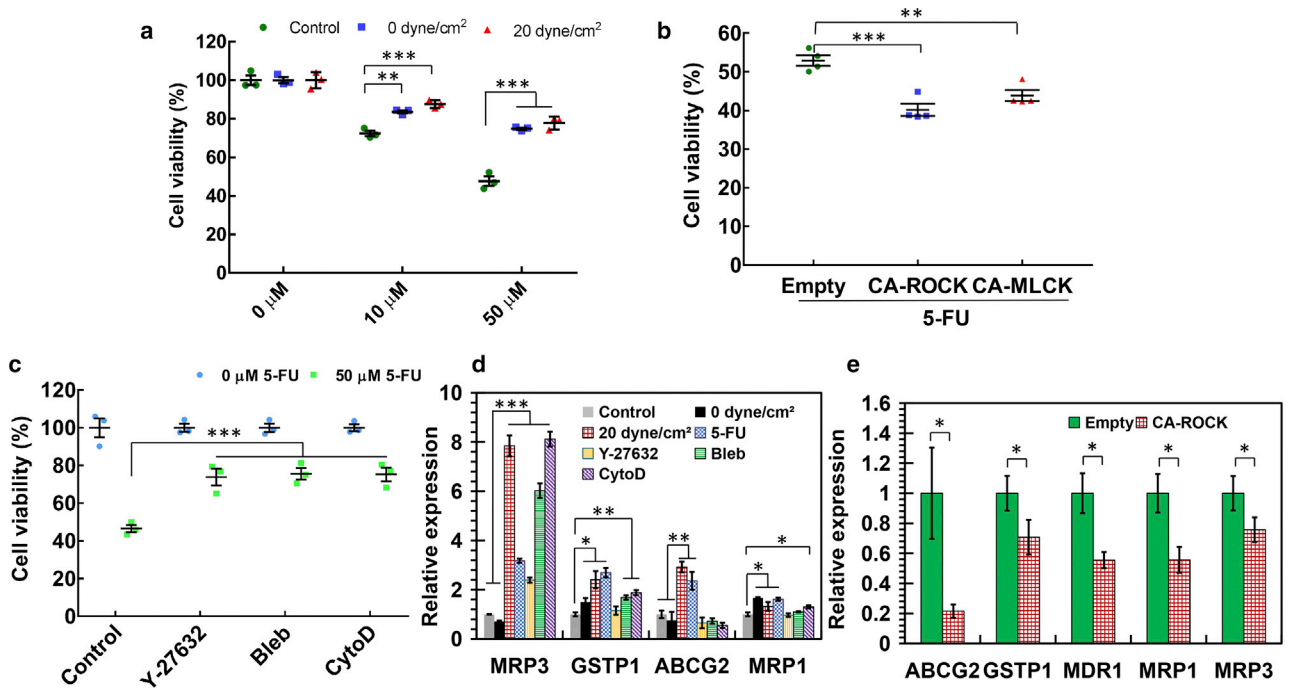

FIGURE 6 Actomyosin activity regulates chemoresistance of suspended tumor cells surviving hemodynamic shear stress. (*a*) Breast cancer cells surviving hemodynamic shear stress or suspension exhibit resistance to chemotherapy drug treatment. MDA-MB-468 cells were circulated under 0 and 20 dyne/cm^2 shear stress for 12 h, respectively. The surviving cells were cultured on glass in the presence of 0, 10, and 50 μM fluorouracil (5-FU) for 24 h, respectively, after which cell viability was examined by MTS assay. The viability was normalized against the value at 0 μM under the same condition. Tumor cells cultured in petri dishes were used as a control; $n = 3$ independent experiments. (*b*) Activating actomyosin in surviving tumor cells suppresses chemoresistance. Cancer cells were transfected with CA-MLCK, CA-ROCK, or empty vector in the absence of doxycycline and then circulated under 20 dyne/cm^2 shear stress for 12 h. The surviving cells were treated with 50 μM 5-FU and 50 ng/mL doxycycline for 24 h, after which cell viability was measured; $n = 4$ independent experiments. (*c*) Inhibiting actomyosin in untreated tumor cells enhances chemoresistance. Tumor cells were pretreated with 2 μM Y-27632, 4 μM blebbistatin, or 0.3 μM cytochalasin D for 24 h and then cultured with 0 or 50 μM 5-FU for another 24 h; $n = 3$ independent experiments. (*d*) Shear stress or inhibition of actomyosin in breast cancer cells upregulates the expressions of genes related to multidrug resistance (MDR). MDA-MB-468 cells were circulated under 0 and 20 dyne/cm^2 shear stress for 12 h or treated with 50 μM 5-FU, 2 μM Y-27632, 4 μM blebbistatin, or 0.3 μM cytochalasin D for 24 h. The expressions of MDR genes were examined by quantitative RT-PCR; $n = 3$ independent experiments. (*e*) Activating actomyosin through ROCK in tumor cells surviving shear stress suppresses the genes related to MDR. Tumor cells were transfected with CA-ROCK plasmids in the absence of doxycycline and then circulated under 20 dyne/cm^2 shear stress for 12 h. The surviving cells were treated with doxycycline for 24 h. The expressions of the genes related to MDR were examined by quantitative RT-PCR; $n = 3$ independent experiments. The statistics were conducted using ANOVA with the post hoc Tukey test in (*a*)–(*d*) and two-tailed Student *t*-test in (*e*). $^*p < 0.05$; $^{**}p < 0.01$; $^{***}p < 0.001$. To see this figure in color, go online.

and contrasts with the effect of shear flow on adhered cells (36). Note that previous studies have shown the reduction of F-actin when cells are in suspension (37). It is known that EMT or hybrid epithelial/mesenchymal phenotype promotes tumor cell malignancy (4–6,38) and cell stiffness is inversely correlated with malignancy (39). The occurrence of EMT or hybrid phenotype and low stiffness in CTCs after shear stress treatment may confer surviving cells enhanced metastatic potential, which may favor the subsequent generation of secondary tumors. In addition, cell adhesion is critical for tumor cell motility and metastasis (40). Although we show that the adhesion of tumor cells surviving fluid shear stress is retarded, the relationship between cell adhesion, EMT or hybrid epithelial/mesenchymal phenotype, and metastatic potential of CTCs needs to be rigorously investigated in the future. Nevertheless, our data demonstrate that hemodynamic shear stress significantly affects the biophysical properties of suspended tumor cells.

Our data, together with several others (21,23,25,26,35,36), show that a subpopulation of suspended tumor cells can survive fluid shear flow. Except the reported oncogenes (25) and nuclear lamin A/C (26), the underlying survival mechanisms, however, remain less understood. We have found that tumor cells surviving shear stress exhibit low stiffness, which is predominantly determined by actomyosin activity (30). It is known that actomyosin is important for cell survival in various contexts, including dissociated embryonic stem cells (41), oxidative stress-induced neuronal apoptosis (42), and disruption of nuclear integrity during apoptosis (43). However, the roles of actomyosin in the survival of suspended CTCs in fluid shear stress remain unclear. Our data show that inhibiting actomyosin significantly enhances the viability of suspended tumor cells in shear flow, whereas activating actomyosin suppresses tumor cell survival. Soft surviving tumor cells and CSCs hold survival advantages in shear flow, whereas activating actomyosin in CSCs inhibits

cell survival. These findings suggest that actomyosin activity regulates the survival of suspended tumor cells in fluid shear stress, which may unveil a new, to our knowledge, mechanism by which a subpopulation of CTCs are able to survive hematogenous dissemination, an essential step toward the generation of metastases. The results that low actomyosin activity or low stiffness promotes tumor cell survival in hemodynamic shear stress are in line with many previous findings. Tumor cells with high metastatic potential exhibit low cell stiffness or actomyosin (39) and hold survival advantages during the metastatic process (6). Increasing actomyosin contractility inhibits the invasion and migration of tumor cells and potentially cell survival in metastasis (44,45). These findings suggest that low actomyosin activity is correlated with malignancy and high survival rate. Consistently, our findings have demonstrated that fibrin-selected CSCs with low stiffness exhibit high self-renewing ability (Fig. S3) (28,29) and high viability in shear flow (Fig. 1 *d*; Fig. S2 *b*). Further, actomyosin regulates tumor cell survival probably through the effects on antiapoptosis genes. In addition, EMT or hybrid epithelial/mesenchymal phenotype appears to occur in surviving tumor cells (Fig. 3; Fig. S4), which may also promote tumor cell survival in shear flow (4,6). Note that the mechanisms by which suspended CTCs sense hemodynamic shear stress remain to be discovered. Nevertheless, these findings may offer a new strategy to eliminate CTCs in blood shear flow by specifically delivering actomyosin-activating compounds into cancer cells through sophisticated drug delivery methods (46).

Metastasis is closely linked with chemoresistance (32). However, the underlying mechanisms have not been fully understood (33,34). In particular, the roles of hemodynamic shear stress and actomyosin-dependent cell mechanics in drug resistance of CTCs remain unclear. Our study shows that tumor cells surviving fluid shear stress exhibit low stiffness and enhanced drug resistance to chemotherapy. Note that there is no significant difference in chemoresistance between tumor cells after suspension and shear stress treatment. The underlying mechanisms need to be further studied. Nevertheless, activating actomyosin in surviving tumor cells suppresses chemoresistance, whereas inhibiting actomyosin in untreated cells enhances drug resistance, suggesting actomyosin may play a regulatory role in chemoresistance of suspended tumor cells. The actomyosin-dependent chemoresistance is possibly mediated by the genes related to MDR. These results are consistent with our previous work that fibrin-selected CSCs are soft and highly chemoresistant (28) and other findings that soft cells separated from the whole tumor cell population are tumorigenic and chemoresistant (47). Note that previous research has indicated the controversial roles of Rho/ROCK signaling in drug resistance (48). Some findings show that overexpressing Rho GDP dissociation inhibitor that negatively regulates Rho activity or inhibiting ROCK signaling mediates cancer cell resistance to chemotherapeutic treatment (49,50), whereas several others report that activating Rho signaling enhances drug resistance in certain types of cancer (51). The effect of ROCK on chemoresistance may be also related to its roles in apoptosis (48). Further, we also show that EMT or hybrid epithelial/mesenchymal phenotype may occur in suspended tumor cells after shear stress treatment. Because EMT or hybrid epithelial/mesenchymal phenotype has been implicated in drug resistance (52,53), it is possible that the chemoresistance ability of surviving tumor cells may be partially mediated by EMT or hybrid phenotype. The relationship between EMT or hybrid epithelial/mesenchymal phenotype, actomyosin activity, and drug resistance of CTCs in fluid shear flow needs to be further investigated in the future. Nevertheless, these findings unveil the critical roles of actomyosin activity in chemoresistance of suspended tumor cells, which may have major implications in the treatment of metastatic tumors.

It is known that CTCs in cancer patients are very rare (1–10 CTCs per mL blood) (2,3). Because of these technical and other challenges, cancer cell lines in suspension have been utilized in this study as an alternative model. Note that they may recapitulate certain aspects but not the bona fide biology of CTCs and differ from primary tumor cells from patients. Further, CTCs reside in a very complexed microenvironment, in which blood cells, immune cells, coagulation factors, and hemodynamic shear flow are present (2,3). This study has investigated the effects of hemodynamic shear stress, but not other factors in blood circulation. The influence of the interactions among various factors on the properties of CTCs has not been examined. Therefore, to extend our current findings to the clinical setting, it is necessary to rigorously test the ideas using patient-derived CTCs or CTC lines in a more sophisticated system better representative of the blood microenvironment.

CONCLUSIONS

In summary, this work reports that the majority of suspended tumor cells in suspension can be eliminated by hemodynamic shear stress. The surviving cells exhibit unique biophysical properties, including retarded cell adhesion, EMT-like or hybrid epithelial/mesenchymal phenotype, and reduced cellular stiffness. Importantly, low actomyosin activity promotes the survival of suspended tumor cells in fluid shear flow and chemoresistance, whereas high actomyosin inhibits tumor cell survival and drug resistance of tumor cells surviving shear stress treatment. These findings unveil the regulatory role of actomyosin activity in the survival of suspended tumor cells in hemodynamic shear stress and chemoresistance, which may have important implications in targeting CTCs and drug resistance in metastasis.

SUPPORTING MATERIAL

Supporting Material can be found online at https://doi.org/10.1016/j.bpj.2019.04.011.

AUTHOR CONTRIBUTIONS

Y.T. conceived the project. Y.T., Y.X., X.C., X.T., and K.L. designed and conducted the experiments, analyzed data, and wrote the manuscript. M.Y., W.C.-S.T., and Y.L. provided plasmids, analyzed data, and commented on the manuscript.

ACKNOWLEDGMENTS

We thank professor Sanjay Kumar (University of California, Berkeley) for the kind gifts of pSLIK CA-MLCK, pSLIK CA-ROCK, and pSLIK-Venus (empty) plasmids, Mr. Tianlong Zhang (The Hong Kong Polytechnic University) for the help in cell stiffness measurement using atomic force microscopy, and professors Larry Ming-cheung Chow (The Hong Kong Polytechnic University) and Zhi-ling Yu (the Hong Kong Baptist University) for the kind gifts of MDA-MB-468, MCF-7, and MDA-MB-453 cells.

Y.T. acknowledges the support from National Natural Science Foundation of China (project no. 11672255), Shenzhen Science and Technology Innovation Commission (project no. JCYJ20170303160515987 and JCYJ20170413154735522), Early Career Scheme from Research Grants Council of the Hong Kong Special Administrative Region, China (PolyU 252094/17E), and the internal grant from The Hong Kong Polytechnic University (1-ZE4Q and 1-ZVJ8).

REFERENCES

1. Valastyan, S., and R. A. Weinberg. 2011. Tumor metastasis: molecular insights and evolving paradigms. *Cell.* 147:275–292.
2. Alix-Panabières, C., and K. Pantel. 2014. Challenges in circulating tumour cell research. *Nat. Rev. Cancer.* 14:623–631.
3. Cristofanilli, M., G. T. Budd, …, D. F. Hayes. 2004. Circulating tumor cells, disease progression, and survival in metastatic breast cancer. *N. Engl. J. Med.* 351:781–791.
4. Alix-Panabières, C., S. Mader, and K. Pantel. 2017. Epithelial-mesenchymal plasticity in circulating tumor cells. *J. Mol. Med. (Berl.).* 95:133–142.
5. Yu, M., A. Bardia, …, S. Maheswaran. 2013. Circulating breast tumor cells exhibit dynamic changes in epithelial and mesenchymal composition. *Science.* 339:580–584.
6. Massagué, J., and A. C. Obenauf. 2016. Metastatic colonization by circulating tumour cells. *Nature.* 529:298–306.
7. Discher, D. E., P. Janmey, and Y. L. Wang. 2005. Tissue cells feel and respond to the stiffness of their substrate. *Science.* 310:1139–1143.
8. Tajik, A., Y. Zhang, …, N. Wang. 2016. Transcription upregulation via force-induced direct stretching of chromatin. *Nat. Mater.* 15:1287–1296.
9. Wang, N., J. D. Tytell, and D. E. Ingber. 2009. Mechanotransduction at a distance: mechanically coupling the extracellular matrix with the nucleus. *Nat. Rev. Mol. Cell Biol.* 10:75–82.
10. Wirtz, D., K. Konstantopoulos, and P. C. Searson. 2011. The physics of cancer: the role of physical interactions and mechanical forces in metastasis. *Nat. Rev. Cancer.* 11:512–522.
11. Kumar, S., and V. M. Weaver. 2009. Mechanics, malignancy, and metastasis: the force journey of a tumor cell. *Cancer Metastasis Rev.* 28:113–127.
12. Lo, K. Y., Y. Zhu, …, Y. S. Sun. 2013. Effects of shear stresses and antioxidant concentrations on the production of reactive oxygen species in lung cancer cells. *Biomicrofluidics.* 7:64108.
13. Luo, C. W., C. C. Wu, and H. J. Ch'ang. 2014. Radiation sensitization of tumor cells induced by shear stress: the roles of integrins and FAK. *Biochim. Biophys. Acta.* 1843:2129–2137.
14. Avvisato, C. L., X. Yang, …, S. W. Byers. 2007. Mechanical force modulates global gene expression and beta-catenin signaling in colon cancer cells. *J. Cell Sci.* 120:2672–2682.
15. Chang, S. F., C. A. Chang, …, J. J. Chiu. 2008. Tumor cell cycle arrest induced by shear stress: roles of integrins and Smad. *Proc. Natl. Acad. Sci. USA.* 105:3927–3932.
16. Trachtenberg, J. E., M. Santoro, …, A. G. Mikos. 2018. Effects of shear stress gradients on Ewing sarcoma cells using 3D printed scaffolds and flow perfusion. *ACS Biomater. Sci. Eng.* 4:347–356.
17. Lee, H. J., M. F. Diaz, …, P. L. Wenzel. 2017. Fluid shear stress activates YAP1 to promote cancer cell motility. *Nat. Commun.* 8:14122.
18. Qazi, H., R. Palomino, …, J. M. Tarbell. 2013. Cancer cell glycocalyx mediates mechanotransduction and flow-regulated invasion. *Integr. Biol.* 5:1334–1343.
19. Rizvi, I., U. A. Gurkan, …, T. Hasan. 2013. Flow induces epithelial-mesenchymal transition, cellular heterogeneity and biomarker modulation in 3D ovarian cancer nodules. *Proc. Natl. Acad. Sci. USA.* 110:E1974–E1983.
20. Ip, C. K., S. S. Li, …, A. S. Wong. 2016. Stemness and chemoresistance in epithelial ovarian carcinoma cells under shear stress. *Sci. Rep.* 6:26788.
21. Fan, R., T. Emery, …, J. Wan. 2016. Circulatory shear flow alters the viability and proliferation of circulating colon cancer cells. *Sci. Rep.* 6:27073.
22. Mitchell, M. J., and M. R. King. 2013. Fluid shear stress sensitizes cancer cells to receptor-mediated apoptosis via trimeric death receptors. *New J. Phys.* 15:015008.
23. Regmi, S., A. Fu, and K. Q. Luo. 2017. High shear stresses under exercise condition destroy circulating tumor cells in a microfluidic system. *Sci. Rep.* 7:39975.
24. Ma, S., A. Fu, …, K. Q. Luo. 2017. Hemodynamic shear stress stimulates migration and extravasation of tumor cells by elevating cellular oxidative level. *Cancer Lett.* 388:239–248.
25. Barnes, J. M., J. T. Nauseef, and M. D. Henry. 2012. Resistance to fluid shear stress is a conserved biophysical property of malignant cells. *PLoS One.* 7:e50973.
26. Mitchell, M. J., C. Denais, …, M. R. King. 2015. Lamin A/C deficiency reduces circulating tumor cell resistance to fluid shear stress. *Am. J. Physiol. Cell Physiol.* 309:C736–C746.
27. Sampieri, K., and R. Fodde. 2012. Cancer stem cells and metastasis. *Semin. Cancer Biol.* 22:187–193.
28. Liu, J., Y. Tan, …, B. Huang. 2012. Soft fibrin gels promote selection and growth of tumorigenic cells. *Nat. Mater.* 11:734–741.
29. Tan, Y., A. Tajik, …, N. Wang. 2014. Matrix softness regulates plasticity of tumour-repopulating cells via H3K9 demethylation and Sox2 expression. *Nat. Commun.* 5:4619.
30. Fletcher, D. A., and R. D. Mullins. 2010. Cell mechanics and the cytoskeleton. *Nature.* 463:485–492.
31. Cross, S. E., Y. S. Jin, …, J. K. Gimzewski. 2007. Nanomechanical analysis of cells from cancer patients. *Nat. Nanotechnol.* 2:780–783.
32. Gonzalez-Angulo, A. M., F. Morales-Vasquez, and G. N. Hortobagyi. 2007. Overview of Resistance to Systemic Therapy in Patients with Breast Cancer. Springer, New York, pp. 1–22.
33. Acharyya, S., T. Oskarsson, …, J. Massagué. 2012. A CXCL1 paracrine network links cancer chemoresistance and metastasis. *Cell.* 150:165–178.
34. Coley, H. M. 2008. Mechanisms and strategies to overcome chemotherapy resistance in metastatic breast cancer. *Cancer Treat. Rev.* 34:378–390.

35. Triantafillu, U. L., S. Park, …, Y. Kim. 2017. Fluid shear stress induces cancer stem cell-like phenotype in MCF7 breast cancer cell line without inducing epithelial to mesenchymal transition. *Int. J. Oncol.* 50:993–1001.

36. Hyler, A. R., N. C. Baudoin, …, E. M. Schmelz. 2018. Fluid shear stress impacts ovarian cancer cell viability, subcellular organization, and promotes genomic instability. *PLoS One.* 13:e0194170.

37. Gerald, N., J. Dai, …, A. De Lozanne. 1998. A role for Dictyostelium racE in cortical tension and cleavage furrow progression. *J. Cell Biol.* 141:483–492.

38. Lecharpentier, A., P. Vielh, …, F. Farace. 2011. Detection of circulating tumour cells with a hybrid (epithelial/mesenchymal) phenotype in patients with metastatic non-small cell lung cancer. *Br. J. Cancer.* 105:1338–1341.

39. Swaminathan, V., K. Mythreye, …, R. Superfine. 2011. Mechanical stiffness grades metastatic potential in patient tumor cells and in cancer cell lines. *Cancer Res.* 71:5075–5080.

40. Cavallaro, U., and G. Christofori. 2001. Cell adhesion in tumor invasion and metastasis: loss of the glue is not enough. *Biochim. Biophys. Acta.* 1552:39–45.

41. Chen, G., Z. Hou, …, J. A. Thomson. 2010. Actin-myosin contractility is responsible for the reduced viability of dissociated human embryonic stem cells. *Cell Stem Cell.* 7:240–248.

42. Wang, Y., Y. Xu, …, J. Kou. 2017. Myosin IIA-related actomyosin contractility mediates oxidative stress-induced neuronal apoptosis. *Front. Mol. Neurosci.* 10:75.

43. Croft, D. R., M. L. Coleman, …, M. F. Olson. 2005. Actin-myosin-based contraction is responsible for apoptotic nuclear disintegration. *J. Cell Biol.* 168:245–255.

44. Wong, S. Y., T. A. Ulrich, …, S. Kumar. 2015. Constitutive activation of myosin-dependent contractility sensitizes glioma tumor-initiating cells to mechanical inputs and reduces tissue invasion. *Cancer Res.* 75:1113–1122.

45. Surcel, A., W. P. Ng, …, D. N. Robinson. 2015. Pharmacological activation of myosin II paralogs to correct cell mechanics defects. *Proc. Natl. Acad. Sci. USA.* 112:1428–1433.

46. Li, J., Y. Ai, …, M. R. King. 2016. Targeted drug delivery to circulating tumor cells via platelet membrane-functionalized particles. *Biomaterials.* 76:52–65.

47. Zhang, W., K. Kai, …, L. Qin. 2012. Microfluidics separation reveals the stem-cell-like deformability of tumor-initiating cells. *Proc. Natl. Acad. Sci. USA.* 109:18707–18712.

48. Wei, L., M. Surma, …, J. Shi. 2016. Novel insights into the roles of rho kinase in cancer. *Arch. Immunol. Ther. Exp. (Warsz.).* 64:259–278.

49. Zhang, B., Y. Zhang, …, E. Shacter. 2005. Rho GDP dissociation inhibitor protects cancer cells against drug-induced apoptosis. *Cancer Res.* 65:6054–6062.

50. Street, C. A., A. A. Routhier, …, B. A. Bryan. 2010. Pharmacological inhibition of Rho-kinase (ROCK) signaling enhances cisplatin resistance in neuroblastoma cells. *Int. J. Oncol.* 37:1297–1305.

51. Sterpetti, P., L. Marucci, …, A. Benedetti. 2006. Cell proliferation and drug resistance in hepatocellular carcinoma are modulated by Rho GTPase signals. *Am. J. Physiol. Gastrointest. Liver Physiol.* 290:G624–G632.

52. Singh, A., and J. Settleman. 2010. EMT, cancer stem cells and drug resistance: an emerging axis of evil in the war on cancer. *Oncogene.* 29:4741–4751.

53. Jolly, M. K., M. Boareto, …, H. Levine. 2015. Implications of the hybrid epithelial/mesenchymal phenotype in metastasis. *Front. Oncol.* 5:155.

Biophysical Journal, Volume *116*

Supplemental Information

Mechanics and Actomyosin-Dependent Survival/Chemoresistance of Suspended Tumor Cells in Shear Flow

Ying Xin, Xi Chen, Xin Tang, Keming Li, Mo Yang, William Chi-Shing Tai, Yiyao Liu, and Youhua Tan

Mechanics and actomyosin-dependent survival and chemoresistance of suspended tumor cells in shear flow

Ying Xin, [1,2] Xi Chen, [1,2] Xin Tang,[2] Keming Li, [1,2] Mo Yang, [2] William Chi-Shing Tai, [2] Yiyao Liu, [3] Youhua Tan[1,2,*]

[1]The Hong Kong Polytechnic University Shenzhen Research Institute, Shenzhen, China

[2]Department of Biomedical Engineering, Hong Kong Polytechnic University, Hong Kong, China

[3]University of Electronic Science and Technology of China, Chengdu, China

*Correspondence: youhua.tan@polyu.edu.hk

Supplementary Materials

Materials and Methods

Cell stiffness measurement by atomic force microscope. Cell stiffness was measured using atomic force microscope (AFM, Bruker Catalyst) with silicon nitride cantilevers (spring constant k: 0.02 to 0.08 N/m) at room temperature. The force F between tip and cell was the product of the cantilever deflection δ and k, i.e., $F = k \times \delta$. Cell Young's modulus E could be measured by fitting force-indentation curves with Sneddon's modification of the Hertzian model for a pyramidal tip, i.e., $F=2/\pi\times\tan(\alpha)\times E/(1-\nu^2)\times d^2$, where d is the indentation depth, α is the half tip angle, ν is 0.5. d was kept within 500 nm at 1 Hz to avoid potential substrate effects and cell damage.

Immunofluorescence staining. Cells after various treatment were cultured on coverslips and fixed with 4% formaldehyde (Sigma Aldrich) for 15 min at room temperature and rinsed with PBS for 3 times to remove excess reagent. 0.1% Triton X-100 (SAFC) in 1% BSA was added to coverslips and incubated for 1 h at room temperature for permeabilization. Primary

antibodies: MnSOD, Bcl2, MRP3 (Abcam) were diluted in 1% BSA and added to coverslips at 4°C overnight. Cells were then incubated with secondary antibodies: Goat Anti-Rabbit IgG H&L (Alexa Fluor® 488) (Abcam) and Goat anti-Mouse IgG (H+L) Highly Cross-Adsorbed Secondary Antibody, Alexa Fluor Plus 488 (Invitrogen) for 1 h at room temperature. The nucleus was then counterstained with DAPI. For F-actin staining, cells were permeabilized with 0.1% Triton X-100 for 5 min. 200 µl of 1x Green Fluorescent Phalloidin Conjugate working solution (Abcam) was then added into fixed cells for 60 min. Cells were rinsed with PBS for 3 times to remove excess dye and placed onto another coverslip with ProLong Gold Antifade Mountant with DAPI (Thermo Fisher Scientific). At least 100 cells/condition were imaged by the inverted fluorescent microscope (Nikon) using FITC and DAPI channel, respectively. Fluorescence intensity was quantified using ImageJ (NIH).

Fibrin gel preparation. Fibrin gels were prepared as previously described (1, 2). Briefly, fibrinogen (Sea Run Holdings Inc) in T7 buffer (pH 7.4, 50 mM Tris, 150 mM NaCl) was mixed with single cell solution into the concentration of 1mg/ml. 50 µl cell/fibrinogen solution was seeded into each well of 96-well plate and mixed with the pre-added 5 µl thrombin (20 U/ml). The plate with fibrin gels was incubated at 37 °C for 10 min. After complete gelation, 150 µl cell culture medium was gently added into each well.

Statistical analysis. Two-tailed Student's t-test or ANOVA analysis was used for the statistics among two or more conditions.

Reference

1. Liu, J., Y. Tan, H. Zhang, Y. Zhang, P. Xu, J. Chen, Y.-C. Poh, K. Tang, N. Wang, and B. Huang. 2012. Soft fibrin gels promote selection and growth of tumorigenic cells. Nat. Mater. 11: 734–41.

2. Tan, Y., A. Tajik, J. Chen, Q. Jia, F. Chowdhury, L. Wang, J. Chen, S. Zhang, Y. Hong, H. Yi, D.C. Wu, Y. Zhang, F. Wei, Y.-C. Poh, J. Seong, R. Singh, L.-J. Lin, S. Doğanay, Y. Li, H. Jia, T. Ha, Y. Wang, B. Huang, and N. Wang. 2014. Matrix softness regulates plasticity of tumour-repopulating cells via H3K9 demethylation and Sox2 expression. Nat. Commun. 5: 4619.

Supplementary Table 1: List of primers

Genes		Quantitative RT-PCR
E-cadherin	5’ primer	TGCCCAGAAAATGAAAAAGG
	3’ primer	GTGTATGTGGCAATGCGTTC
Fibronectin	5’ primer	CAGTGGGAGACCTCGAGAAG
	3’ primer	TCCCTCGGAACATCAGAAAC
Twist	5’ primer	GGAGTCCGCAGTCTTACGAG
	3’ primer	TCTGGAGGACCTGGTAGAGG
Vimentin	5’ primer	ACTCCCTCTGGTTGATAC
	3’ primer	ATCGTGATGCTGAGAAGT
Bcl2	5’ primer	GTCATGTGTGTGGAGAGCGTCAACC
	3’ primer	CCAGGGCCAAACTGAGCAGAGTC
SOD2	5’ primer	GCACATTAACGCGCAGATCA
	3’ primer	AGCCTCCAGCAACTCTCCTT
ABCG2	5’ primer	TGGCTGTCATGGCTTCAGTA
	3’ primer	GCCACGTGATTCTTCCACAA
GAPDH	5’ primer	GCGACACCCACTCCTCCACCTTT
	3’ primer	TGCTGTAGCCAAATTCGTTGTCATA
GSTP1	5’ primer	TCTACGCAGCACTGAATCCG
	3’ primer	GGAGCTGCCCATACAGACAA
MDR1	5’ primer	CCCATCATTGCAATAGCAGG
	3’ primer	GTTCAA ACTTCTGCTCCTGA
MRP1	5’ primer	AGGCCTACTACCCCAGCATT
	3’ primer	CAGTCTCTCCACTGCCACAA
MRP3	5’ primer	CTTAAGACTTCCCCTCAACATGC
	3’ primer	GGTCAAGTTCCTCTTGGCTC

Supplementary Figures

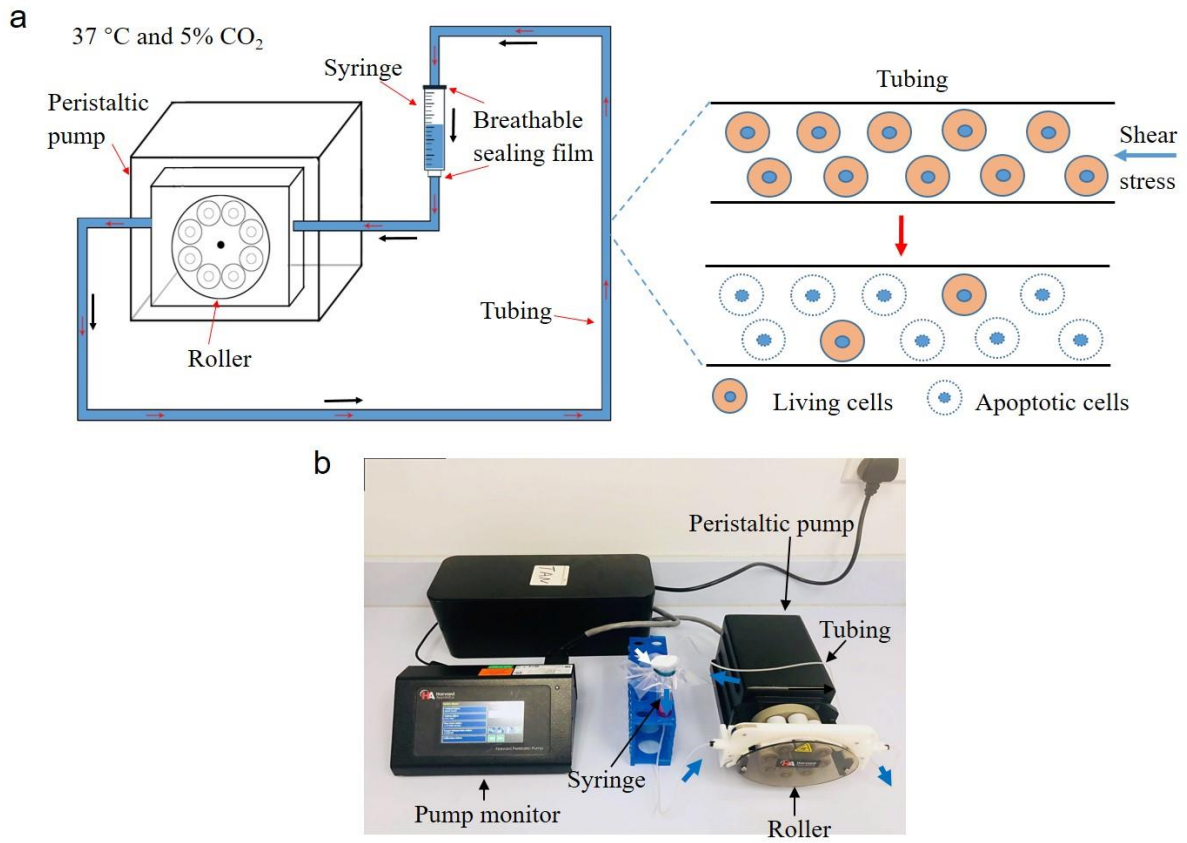

FIGURE S1 The circulatory system developed in this study. (*a*) The schematic of the circulatory microfluidic system. The system was composed of a peristaltic pump (P-230, Harvard Apparatus), a silicone micro-tubing (0.51 mm in diameter and 1.5 m in length), and a syringe as cell solution reservoir. This system could generate pulsatile flow, which mimicked the hemodynamic shear stress in blood circulation. Tumor cells in suspension were treated by various magnitudes of shear stress and circulation duration. (b) The image of the experimental system.

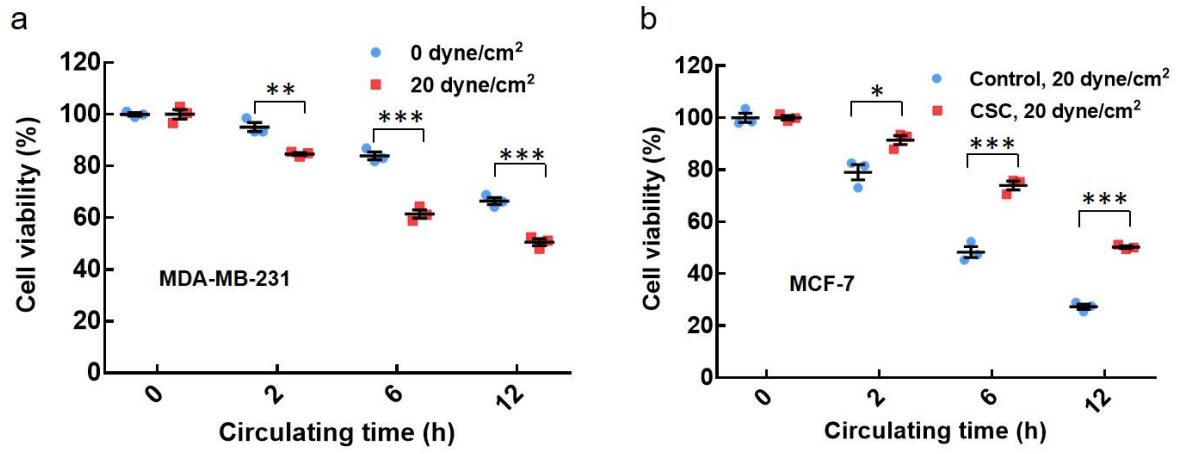

FIGURE S2 The survival of breast cancer cells and CSCs in fluid shear stress. (a) The viability of MDA-MB-231 cells decreases with shear stress and circulation duration. Suspended tumor cells were treated in the circulatory system under 0 and 20 dyne/cm^2 shear stress for 0, 2, 6, and 12 h, respectively. The viability of treated cells was measured by MTS assay and was normalized by the data at 0 h under the same treatment. n=3 independent experiments. (b) CSCs from MCF-7 exhibit higher viability than bulk tumor cells in shear stress. CSCs were acquired by culturing MCF-7 cells in soft fibrin gels for 7 days. Suspended CSCs and MCF-7 cells were then treated in 20 dyne/cm^2 shear stress for various durations, when cell viability was measured. n=3 independent experiments. *, $p<0.05$; **, $p<0.01$; ***, $p<0.001$.

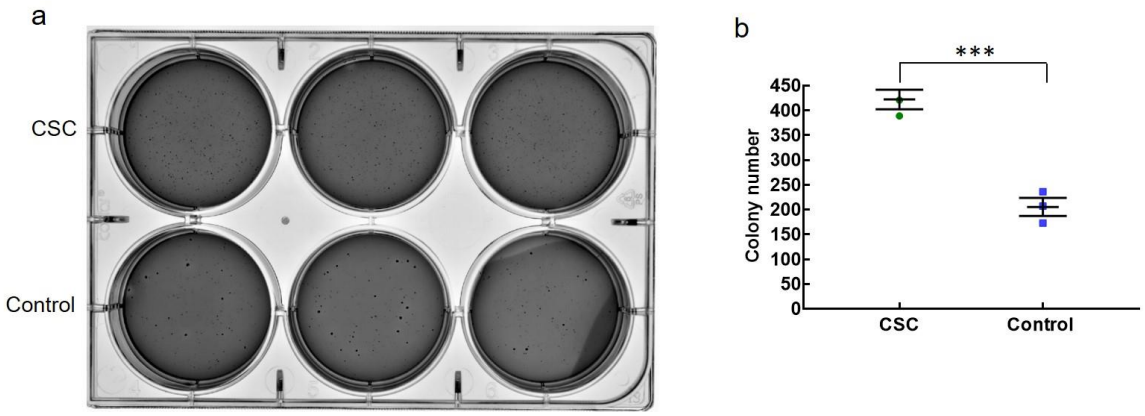

FIGURE S3 Fibrin-selected breast cancer cells are CSCs with high self-renewal. MCF7 cells were cultured in soft fibrin gels for 7 days. These fibrin-selected cells (CSCs) and control cells were cultured in soft agar for 10 days. The micrographs of the plates were shown in (a) and the colony number was quantified in (b). n=3 independent experiments. ***, $p<0.001$.

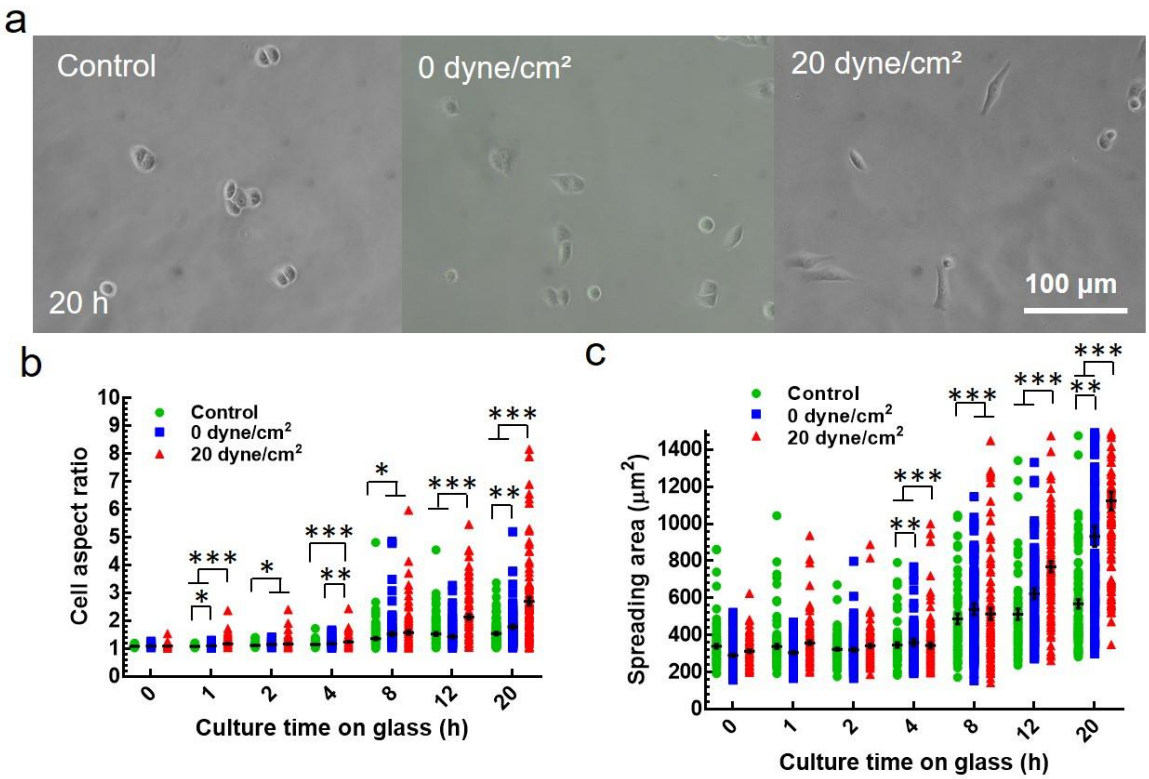

FIGURE S4 Shear stress promotes mesenchymal phenotype in MCF-7 cells. (a) Representative images of MCF-7 cells after shear stress treatment. MCF-7 cells were treated under 0 and 20 dyne/cm^2 shear stress and then cultured on collagen-coated glass. Tumor cells cultured in petri dishes were used as control. Cell images were taken at the indicated time points. Scale bar: 100 μm. (b, c) Fluid shear stress promotes elongated morphology and spreading of MCF-7 cells. The aspect ratio (b) and spreading area (c) of the treated tumor cells in (a) were quantified by ImageJ (n>95). n=2 independent experiments. *, $p<0.05$; **, $p<0.01$; ***, $p<0.001$.

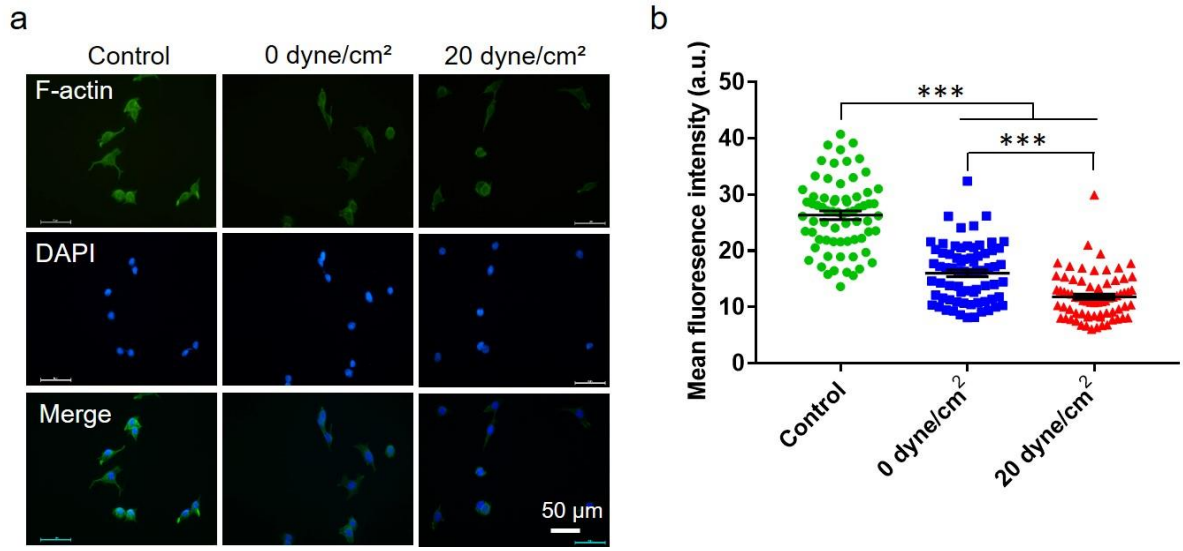

FIGURE S5 MCF-7 cells surviving shear stress exhibit low F-actin and cell stiffness. (a) Immunofluorescence imaging of F-actin in MCF-7 cells after shear stress treatment. MCF-7 cells were treated under 0 and 20 dyne/cm^2 shear stress for 12 h and then plated on glass for 10 h, when F-actin was examined by immunofluorescence staining. The nucleus was counterstained with DAPI. Scar bar: 50 μm. (b) Surviving tumor cells show much lower F-actin. F-actin assembly in (a) was quantified (n>100). a.u.: arbitrary unit. n=2 independent experiments. *, p<0.05; **, p<0.01; ***, p<0.001.

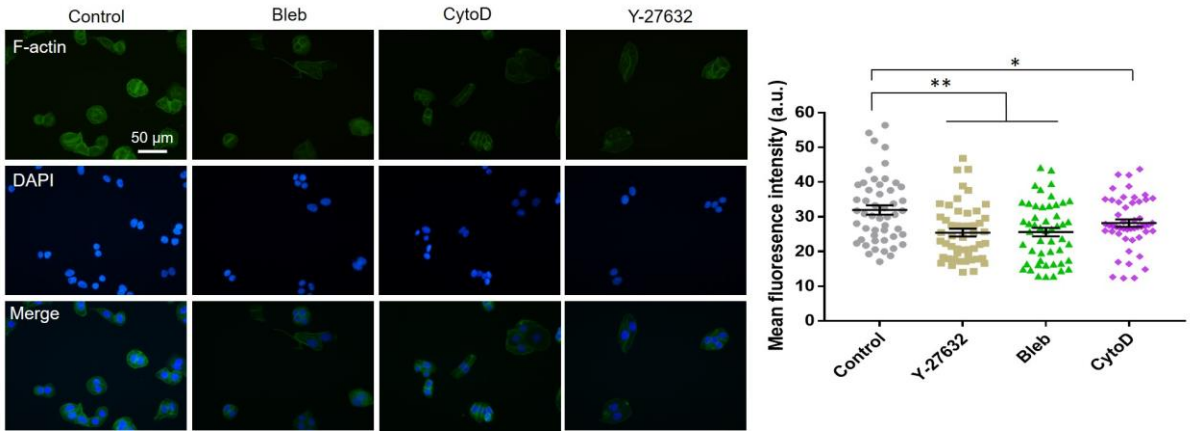

FIGURE S6 Pharmacologically inhibiting actomyosin decreases F-actin assembly. Breast cancer cells MDA-MB-468 were treated with 4 μM myosin II inhibitor blebbistatin, 2 μM ROCK inhibitor Y-27632, and 0.3 μM F-actin inhibitor cytochalasin D. The F-actin assembly in these cells were then examined by immunofluorescence staining and the nucleus was counterstained with DAPI. The fluorescence intensity was quantified by ImageJ (right panel). n> 50 cells. Scale bar: 50 μm. n=2 independent experiments. *, $p<0.05$; **, $p<0.01$.

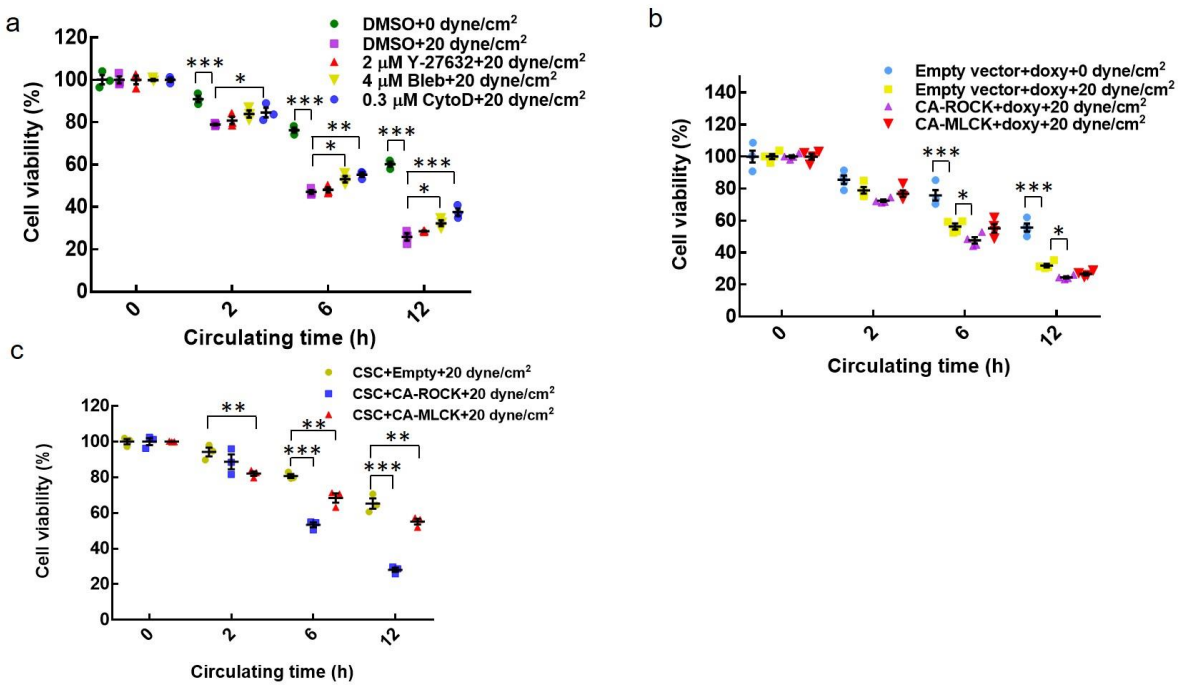

FIGURE S7 Actomyosin regulates the survival of MCF-7 cells in fluid shear stress. (a) Inhibiting actomyosin activity through myosin or actin but not ROCK enhances cell viability in shear flow. MCF-7 cells were treated with 2 μM Y-27632, 4 μM blebbistatin (Bleb), or 0.3 μM cytochalasin D (CytoD) for 48 h and then circulated under 0 or 20 dyne/cm^2 shear stress for the indicated durations, when cell viability was measured by MTS assay. Activating actomyosin in MCF-7 cells through ROCK but not MLCK (b) and MCF-7 CSCs through both MLCK and ROCK (c) suppresses the survival of suspended tumor cells in fluid shear flow. MCF-7 were transfected with CA-MLCK or ROCK or empty vector in the presence of doxycycline and then circulated under 20 dyne/cm^2 shear stress with doxycycline. CSCs were obtained by culturing these modified MCF-7 cells in soft fibrin gels for 5 days without doxycycline, where doxycycline was added at day 6 and 7 to activated ROCK or MLCK. These CSCs were then treated under 20 dyne/cm^2 shear stress with doxycycline for the indicated durations, when cell viability was measured. n=3 independent experiments. *, $p<0.05$; **, $p<0.01$; ***, $p<0.001$.

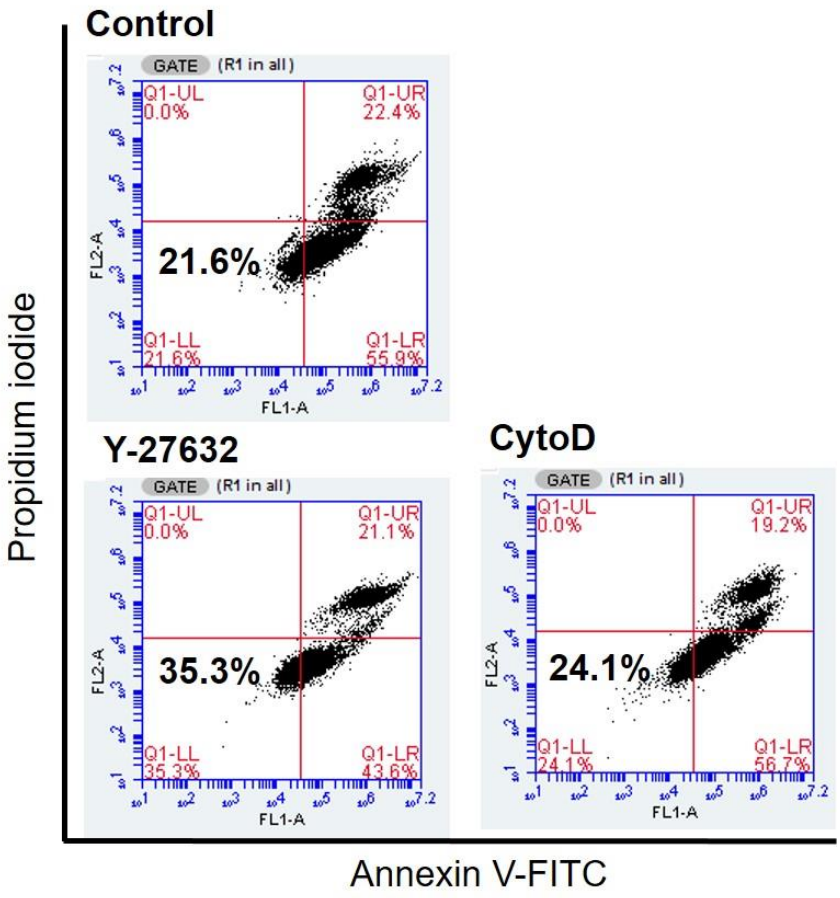

FIGURE S8 Pharmacologically inhibiting actomyosin increases the survival of tumor cells in fluid shear flow. Breast cancer cells MDA-MB-468 were treated with 2 μM ROCK inhibitor Y-27632 or 0.3 μM F-actin inhibitor cytochalasin D for 48 h and then circulated under 20 dyne/cm^2 shear stress for 12 h. Control cells treated with DMSO were used as a control. Cell survival was examined by Annexin V assay. The value in the flow cytometry figure represents the fraction of viable cells. n=2 independent experiments.

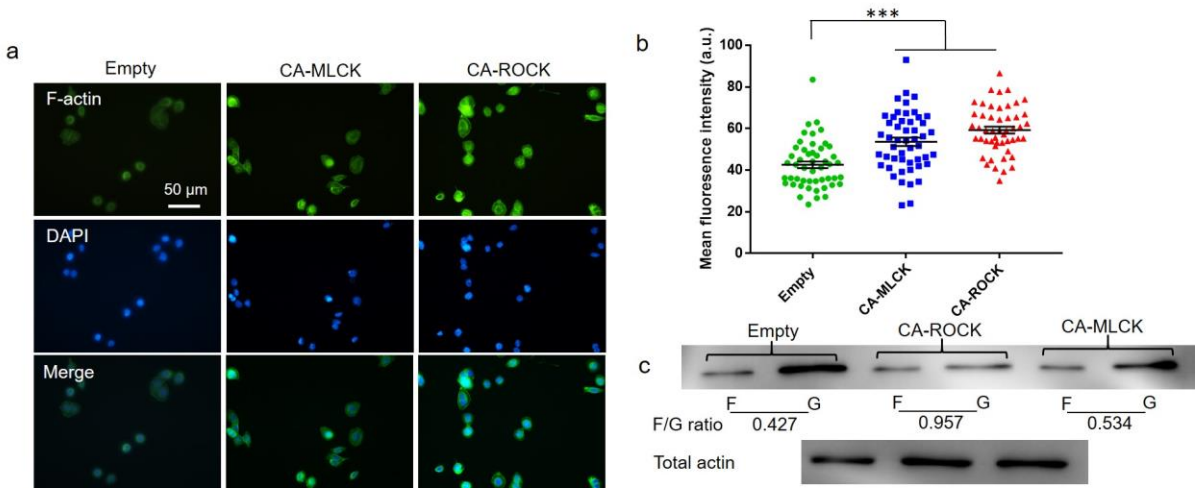

FIGURE S9 Overexpressing MLCK/ROCK enhances F-actin assembly. (a) Immunofluorescence imaging of F-actin in breast cancer cells with overexpression of MLCK or ROCK. MDA-MB-468 cells were transfected with constitutive active (CA) mutants of MLCK or ROCK in the presence of doxycycline, which could activate the plasmids. The F-actin assembly in these cells was then examined by immunofluorescence staining and the nucleus was counterstained with DAPI. Scale bar: 50 μm. (b) Quantification of F-actin assembly. The fluorescence intensity in (a) was quantified by ImageJ (right panel). n>80 cells. ***, $p<0.001$. (c) Immunoblotting of G-actin and F-actin in tumor cells with overexpression of MLCK or ROCK. MDA-MB-468 cells with overexpression of CA-MLCK or CA-ROCK were analyzed for the expression of G-actin and F-actin by western blotting. The values represent the F-actin/G-actin ratio. The level of total actin was used as loading control. n=2 independent experiments.

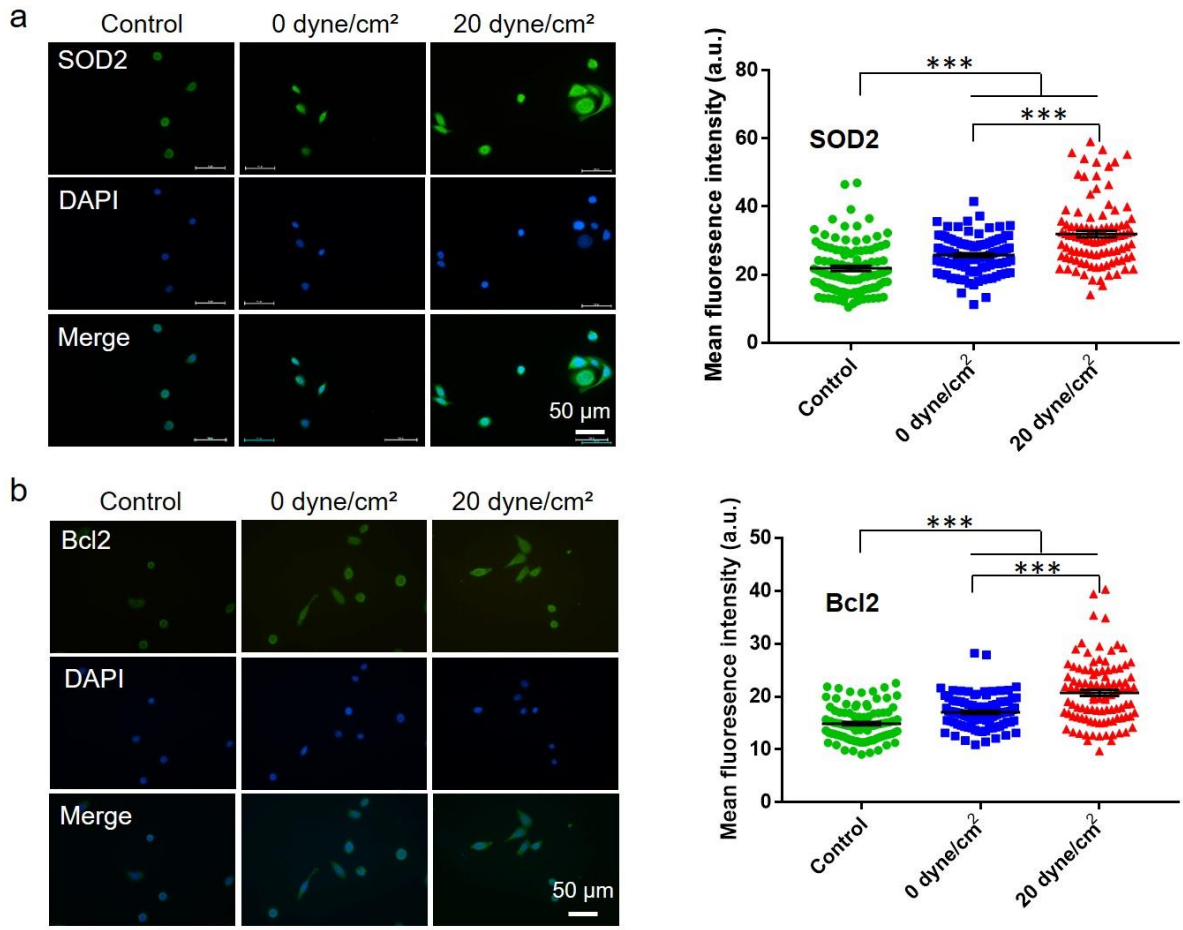

FIGURE S10 Hemodynamic shear stress up-regulates the expression of SOD2 and Bcl2. MDA-MB-468 cells were treated under 0 and 20 dyne/cm^2 shear stress for 12 h and then plated on glass for the analysis of SOD2 (a) and Bcl2 (b) by immunofluorescence staining. The nucleus was counterstained with DAPI. Tumor cells cultured on glass were used as control. The fluorescence intensity was quantified by ImageJ (right panel). At least 100 cells were used for each condition. n=2 independent experiments. Scale bar: 50 μm. ***, $p<0.001$.

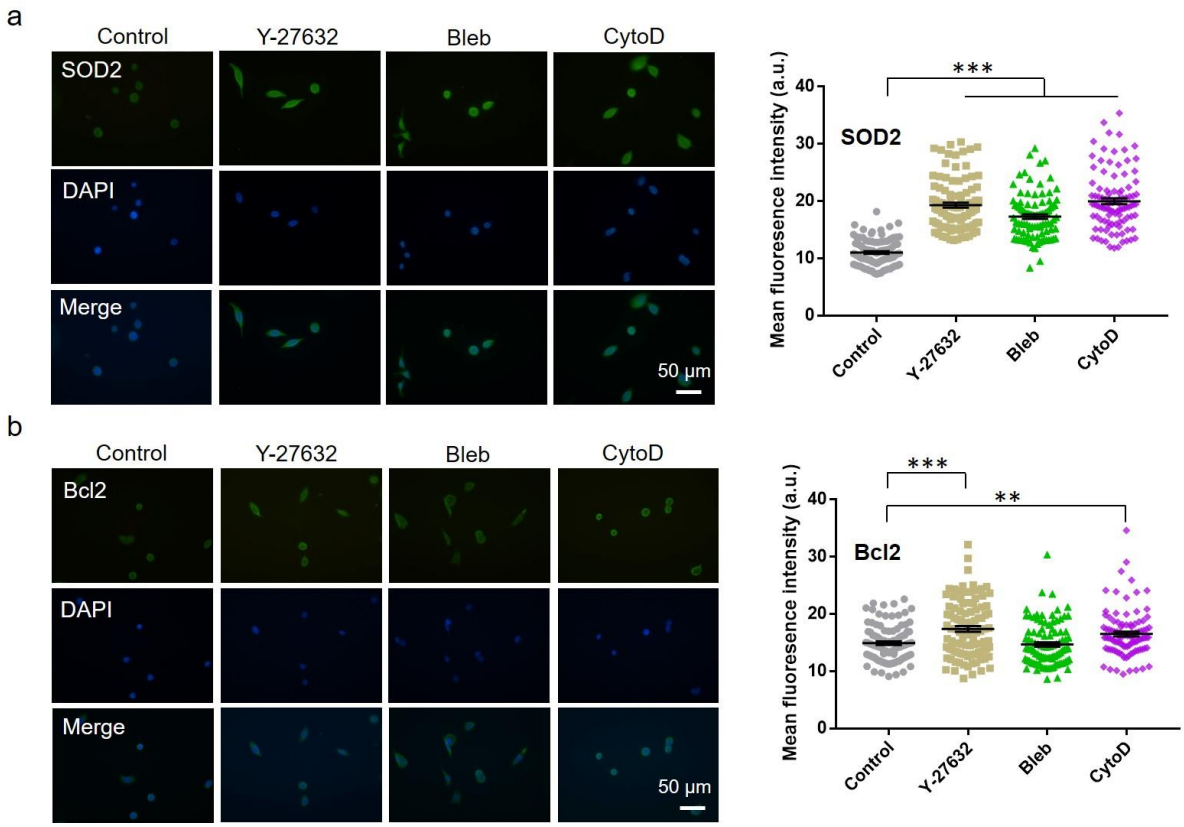

FIGURE S11 Inhibiting actomyosin up-regulates the expression of SOD2 and Bcl2. MDA-MB-468 cells were treated with 2 μM Y-27632, 4 μM blebbistatin, or 0.3 μM cytochalasin D for 48h and then analyzed for the expression of SOD2 (a) and Bcl2 (b) by immunofluorescence staining. Tumor cells treated with DMSO were used as control. The nucleus was counterstained with DAPI. The fluorescence intensity was quantified by ImageJ (right panel). At least 100 cells were used for each condition. n=2 independent experiments. Scale bar: 50 μm. **, $p<0.01$; ***, $p<0.001$.

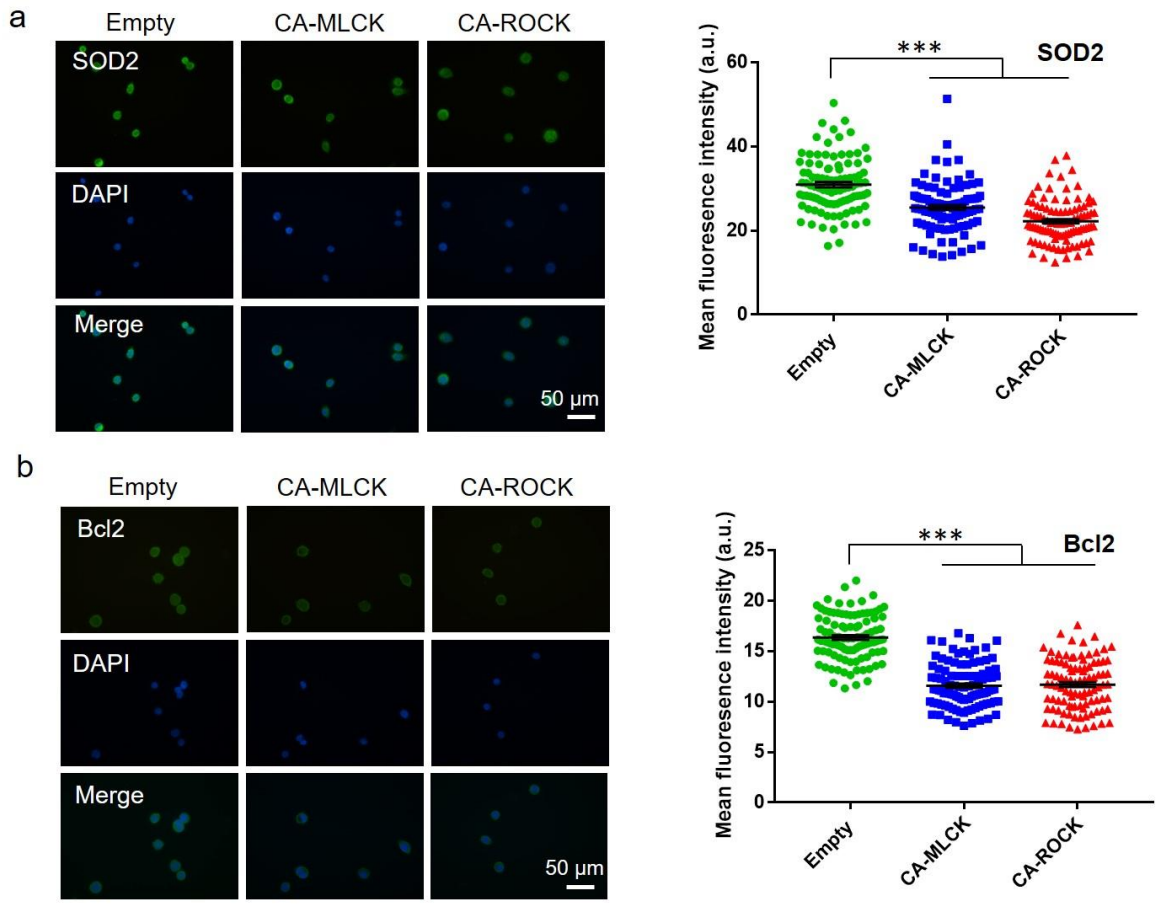

FIGURE S12 Activating actomyosin down-regulates the expression of SOD2 and Bcl2. MDA-MB-468 cells were transfected with CA-MLCK or ROCK in the presence of doxycycline for 48h and then analyzed for the expression of SOD2 (a) and Bcl2 (b) by immunofluorescence staining. Tumor cells transfected with empty vectors were used as control. The nucleus was counterstained with DAPI. The fluorescence intensity was quantified by ImageJ (right panel). At least 100 cells were used for each condition. n=2 independent experiments. Scale bar: 50 μm. ***, $p<0.001$.

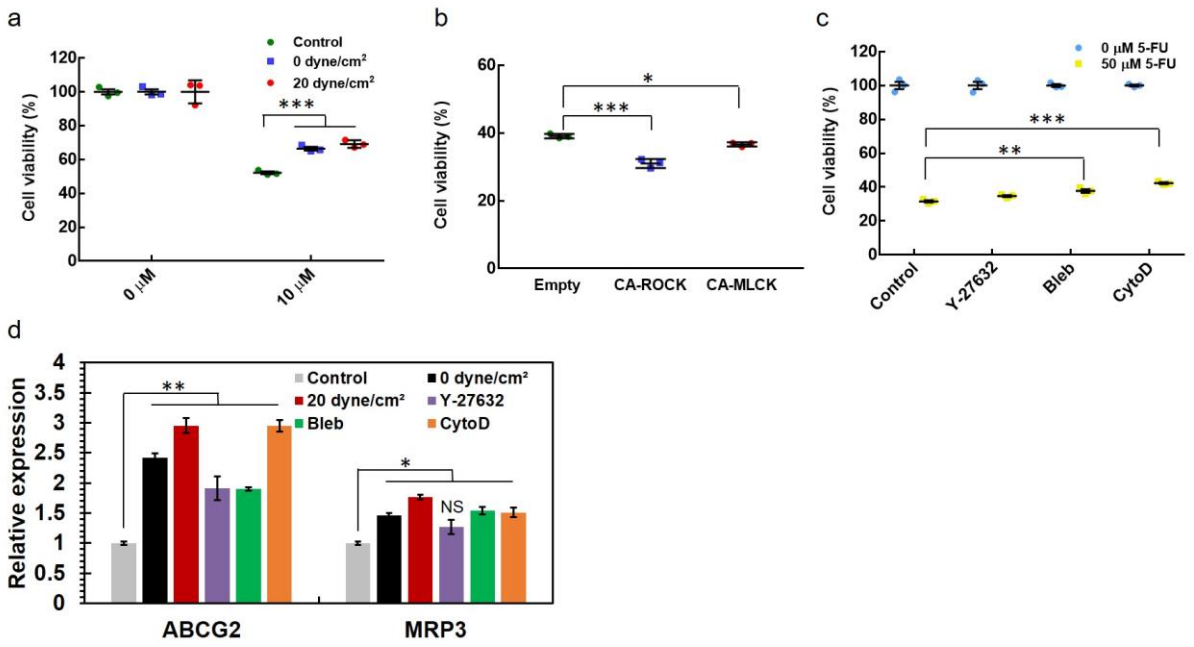

FIGURE S13 Tumor cells surviving fluid shear stress exhibit chemoresistance dependent on actomyosin. (a) Tumor cells surviving suspension or shear stress show enhanced drug resistance to chemotherapy. MCF-7 cells were circulated under 0 and 20 dyne/cm^2 shear stress for 12 h and then plated on glass with 0 or 10 μM 5-FU for 24 h. Cell viability was measured by MTS assay. The viability was normalized against to the value at 0 μM under the same condition. Tumor cells cultured in petri dishes were used as a control. n=3 independent experiments. (b) Activating actomyosin inhibits chemoresistance of surviving tumor cells. MCF-7 cells were transfected with CA-MLCK, CA-ROCK, or empty vector without doxycycline and then circulated under 20 dyne/cm^2 shear stress for 12 h. The surviving cells were treated with 50 μM 5-FU and doxycycline for 24 h, when cell viability was measured. n=3 independent experiments. (c) Inhibiting actomyosin in control cells enhances chemoresistance. MCF-7 cells were treated with 2 μM Y-27632, 4 μM blebbistatin, or 0.3 μM cytochalasin D for 24 h and then cultured with 0 or 50 μM 5-FU for another 24 h, when cell viability was measured. n=3 independent experiments. (d) Shear stress or inhibition of actomyosin in breast cancer cells up-regulates the expressions of genes related to multidrug

resistance. MCF-7 cells surviving 0 and 20 dyne/cm^2 shear stress in (a) or pre-treated by Y-27632, blebbistatin, or cytochalasin D in (c) were used for the analysis of genes related to multidrug resistance by quantitative RT-PCR, including ABCG2 and MRP3. NS: no significant difference vs 'Control'. n=3 independent experiments. *, $p<0.05$; **, $p<0.01$; ***, $p<0.001$.

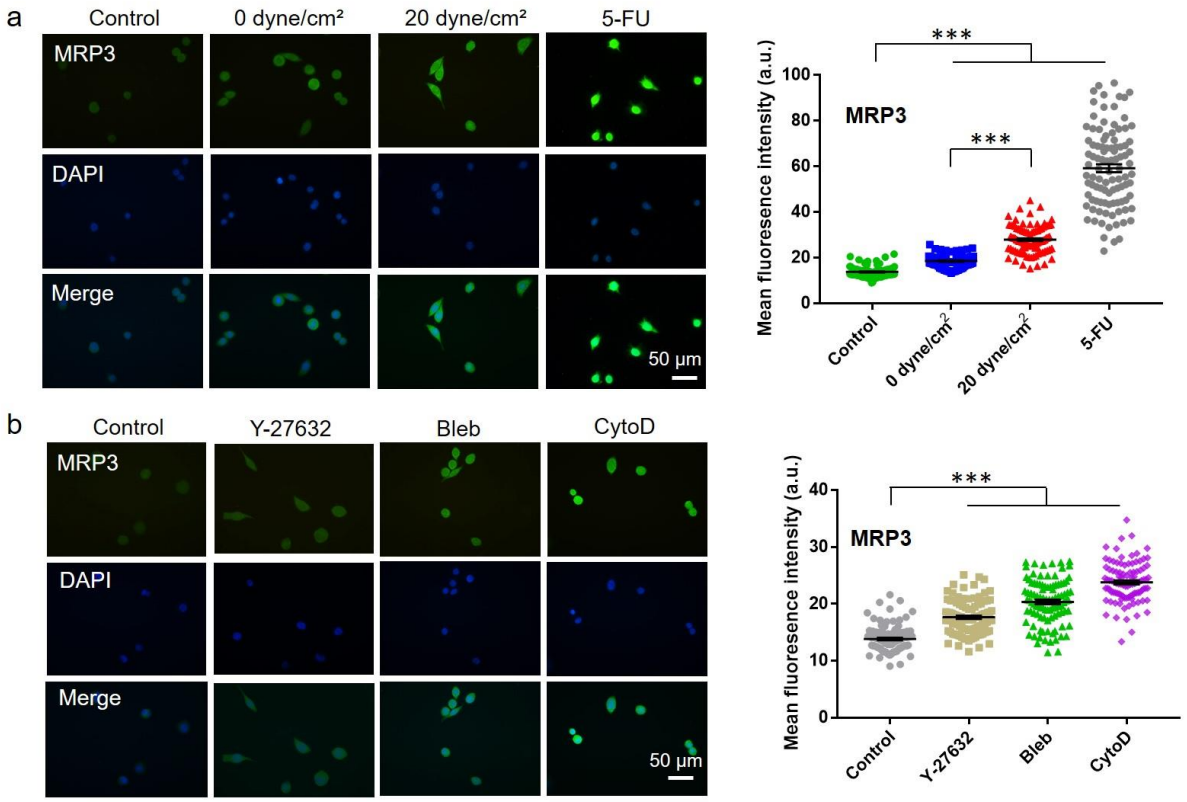

FIGURE S14 Hemodynamic shear stress or inhibiting actomyosin up-regulates MRP3 expression. MDA-MB-468 cells were circulated under 0 and 20 dyne/cm^2 shear stress for 12 h (a) or treated with 50 μM 5-FU, 2 μM Y-27632, 4 μM blebbistatin, or 0.3 μM cytochalasin D (b) for 24 h. The expression of MRP3 was analyzed by immunofluorescence staining. Tumor cells treated with DMSO were used as control. The nucleus was counterstained with DAPI. The fluorescence intensity was quantified by ImageJ (right panel). At least 100 cells were used for each condition. n=2 independent experiments. Scale bar: 50 μm. ***, $p<0.001$.

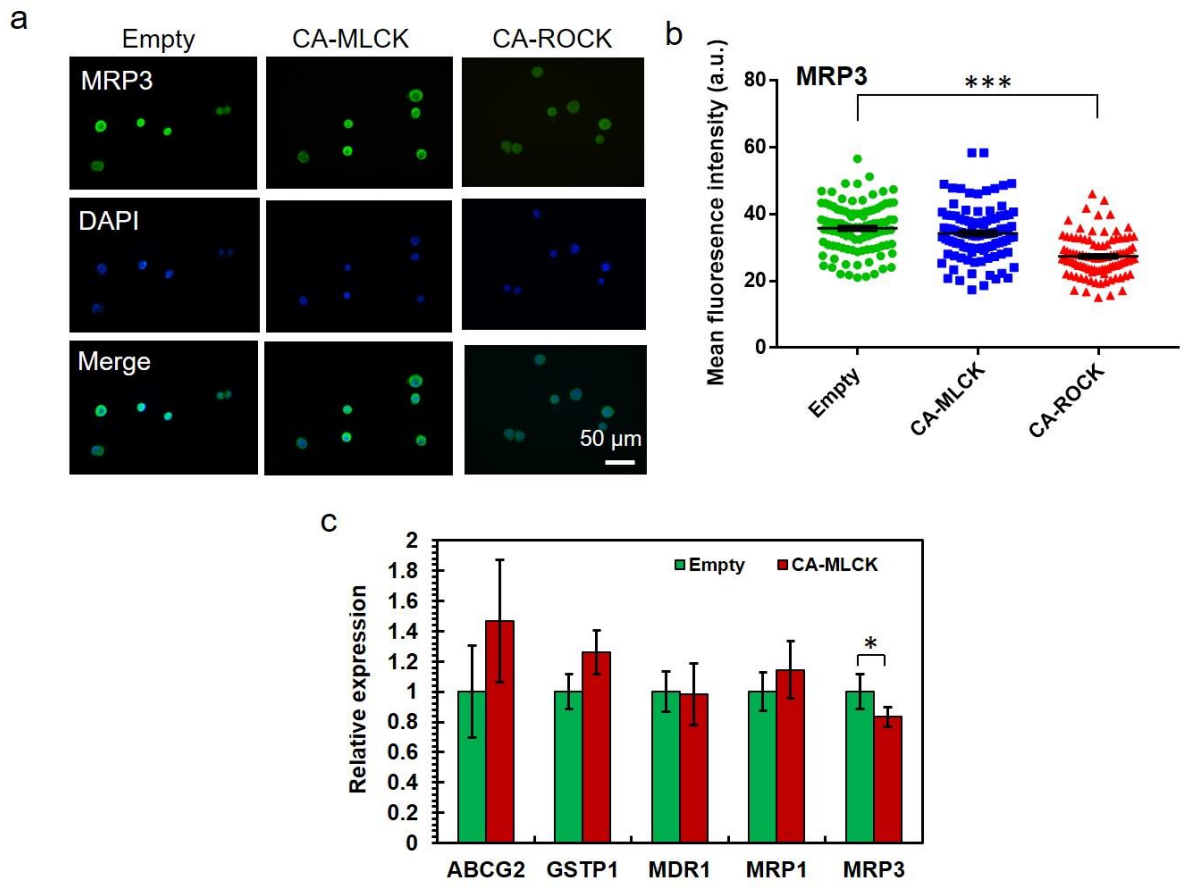

FIGURE S15 Activating actomyosin through ROCK but not MLCK down-regulates the genes related to multidrug resistance. (a) Immunofluorescence imaging of MRP3 in tumor cells with overexpression of MLCK or ROCK. MDA-MB-468 cells were transfected with CA-MLCK or CA-ROCK in the presence of doxycycline for 48 h and then analyzed for the expression of MRP3 by immunofluorescence staining. Tumor cells transfected with empty vectors were used as control. The nucleus was counterstained with DAPI. Scale bar: 50 μm. (b) Quantification of fluorescence intensity in (a). The fluorescence intensity was quantified by ImageJ. At least 100 cells were used for each condition. n=2 independent experiments. (c) Activating MLCK in surviving tumor cells has no significant effects on the genes related to multidrug resistance. MDA-MB-468 cells were transfected with CA-MLCK plasmids in the absence of doxycycline and then circulated under 20 dyne/cm^2 shear stress for 12 h. The surviving cells were treated

with doxycycline for 24 h. The expressions of the genes related to multidrug resistance were examined by quantitative RT-PCR. n=3 independent experiments. *$p<0.05$; ***, $p<0.001$.